Brain Research Reviews, 6 (1983) 139–171
Elsevier

Cellular Bases of Hippocampal EEG in the Behaving Rat

GYÖRGY BUZSÁKI*, LAI-WO S. LEUNG and CORNELIUS H. VANDERWOLF**

Department of Psychology, University of Western Ontario, London, Ont. N6A 5C2 (Canada)

(Accepted May 3rd, 1983)

Key words: Hippocampus — EEG — unit activity — urethane — atropine — entorhinal cortex — septum — fornix — theta model

CONTENTS

* On leave of absence from the Department of Physiology, University Medical School, H-7643 Pécs, Hungary.
** Send reprint requests to this author.

1. INTRODUCTION

The goal of investigating the neuronal mechanisms of the hippocampal EEG is twofold. First, understanding the cellular and neurochemical events underlying the slow waves of the relatively simple archicortex will bring us significantly closer to the understanding of the neocortical EEG[38,46,82], which in turn would help overcome the many problems in clinical electroencephalography. Second, 'decomposition' of the slow waves into spatiotemporal relationships of cell-group activity will provide a better basis for hypotheses about the function of the structure[63,64,81,100].

The most characteristic EEG type of the hippocampus is its rhythmical slow activity (RSA, theta pattern)[55,57,67,133], which is a high amplitude regular EEG pattern occurring particularly in non-primate mammals. Despite extensive investigation, the neuronal mechanisms of hippocampal RSA are not well understood. Current knowledge about hippocampal RSA generation, based mainly on data from anesthetized animals, could be summarized as follows. The septal cholinergic pacemaker input[12,54,88,92,102] is fed into the parallel laminar circuits of the hippocampus[49,50,83,109,127,130] and rhythmically excites pyramidal and granule cells[19,48,67,102,125]. Axon collaterals of the principal neurons (pyramidal and granule cells) then excite, also rhythmically, inhibitory interneurons[33,52,104,107,117,118,124] which in turn inhibit the principal cells in a periodical fashion[3,8,9,13,17,66,120]. This periodic excitation–inhibition would result in rhythmical fluctuations of the membrane potential in a large population of the pyramidal and granule cells[13,19,48,51,67] which linearly summate[48,61,82] to result in extra-cellular field RSA.

Several recent findings indicate, however, that the 'septo-hippocampal excitation recurrent inhibition' model[67] is inadequate. First, activation of the septo-hippocampal circuitry[32,84,91,97,115,128], as reflected by the appearance of RSA, by sensory stimulation, hypothalamic and brainstem stimulation or by stimulation of peripheral nerves was accompanied by a *decrease* in the discharge frequency of pyramidal cells[13,39,42,55,58,59,65,86]. Interneurons, on the other hand were found to increase their firing rate[13,23,26,34,44]. Also, during paradoxical sleep in the rat[89,94,101], cat[15] and man[96], the spontaneous activity of pyramidal cells was found to be the lowest among behavioral states, accompanied by the highest amplitude and most regular RSA in the cat and the rat. Second, in a recent computer model the empirically found RSA laminar profiles could not be simulated by proximal (i.e. close to soma, reflecting the major terminating site of septal afferents[32,47,84,91,92,97,128]) excitation of either pyramidal cells alone or in combination with the granule cells[61]. Third, although the septo-hippocampal input may be exclusively cholinergic[84] in the awake rat and rabbit, cholinergic blockade is not capable of abolishing all RSA[70,134].

In the present experiments we examined the relationship between physiologically identified cell types of the hippocampus and slow waves in the behaving rat. Since no specific hypotheses have been put forward yet for the cellular mechanisms of the large amplitude irregular waves (LIA) and fast activity we extended our investigations to these EEG patterns as well. Unitary discharges were quantitatively related to EEG patterns derived from both the movable microelectrode and a stationary reference electrode placed in the CA1 pyramidal layer. In order to make the successively obtained unit-EEG correlations comparable, identical behavioral states were assured by an operant paradigm. The results allowed us to construct a new model of RSA generation based on feed-forward inhibition from the septum and direct excitation from the entorhinal cortex[6,10,11,90,121].

2. METHODS

2.1. *Subjects*

The experimental subjects were 43 male Long-Evans rats weighing 300–400 g. They were housed individually and allowed ad libitum access to food. Water was available until behavioral training began, after which the rats received water only as reinforcement in the testing apparatus.

2.2. *Experimental chamber*

The experimental chamber was a 30 cm × 40 cm × 35 cm box with an open top. A modified Wahman activity wheel (30 cm in diameter) was attached to one of the longer sides. The front side was made of glass to allow behavioral observation. A drinking tube,

5 cm above the floor, protruded from the wall opposite to the activity wheel. A light source and a phototransistor were fixed on the front and back walls, respectively, in order to detect the rat in the vicinity of the drinking tube ($\leq$ 5 cm). A miniature loudspeaker, placed 6 cm above the drinking tube, served to deliver the 500 Hz tone discriminative stimulus (S_D).

2.3. *Training procedure*

The rats were water deprived for 24 h and were placed in the chamber. In the first session half a turn of the activity wheel switched on S_D which was terminated by the rat's crossing the lightbeam. Concurrently with the termination of S_D 0.5 ml water was automatically delivered into the drinking tube. On successive sessions the number of wheel revolutions for switching on S_D was gradually increased. The final criterion (4–8 turns) varied from subject to subject. Some rats were simply placed in the chamber without any training and their spontaneous behavior was compared with the physiological events.

2.4. *Surgery*

Following criterion performance the rats were anesthetized with Nembutal (45 mg/kg) and placed in a stereotaxic apparatus with the skull level (bregma and lambda in the same horizontal plane). A pair of 150 μm stainless steel electrodes with 1.0 mm tip separation was placed in the right angular bundle (AP = 7.0 mm from bregma, L = 4.5 mm from midline and 3.5 mm below the dura) to stimulate the perforant path afferents to the dentate gyrus[47,90,121,122] (Fig. 1). A single 62 μm wire was positioned in the stratum oriens/pyramidale of CA1 through a 4 mm hole drilled over the right hippocampus. The center of the hole was 3.0 mm posterior to bregma and 2.7 mm from the midsagittal suture. A nylon tube (5.0 mm inner diameter) was fixed above the hole and served as a receptacle for a microdrive for moving tungsten microelectrodes which were etched to give an impedance of 2–20 MΩ. One turn of the microdrive advanced the microelectrode 330 μm. Three 75 μm steel electrodes were implanted in the left hippocampus. One was positioned in the CA3 pyramidal layer (AP = 3.0, L = 3.0, V = 3.5) and served to stimulate the commissural paths to the contralateral dentate gyrus[72,73,108,139] and CA1 region[16,60,74,129,130]. The associational input (Schaffer collaterals[113]) to the right CA1 region was activated indirectly by stimulating through an electrode placed in the left stratum oriens of CA1 (AP = 3.1, L = 2.4, V = 1.9) and backfiring the contralateral CA3 pyramidal cells[25,129]. The third electrode was placed either in the hilus (AP = 3.0, L = 2.5, V = 3.5) or in the molecular layer of the dentate gyrus (AP = 3.0, L = 2.5, V = 2.8). The accuracy of stereotaxic implantation was increased by observing the evoked field responses. Two stainless steel screws driven into the bone over the cerebellum served as indifferent and ground electrodes, respectively. The electrodes were soldered to male pins and the assembly was fixed to the skull with dental cement. In 9 rats an additional wire (150 μm) with a 2 mm uninsulated tip was inserted into the medial septum (AP = 1.0, L = 0.0, V

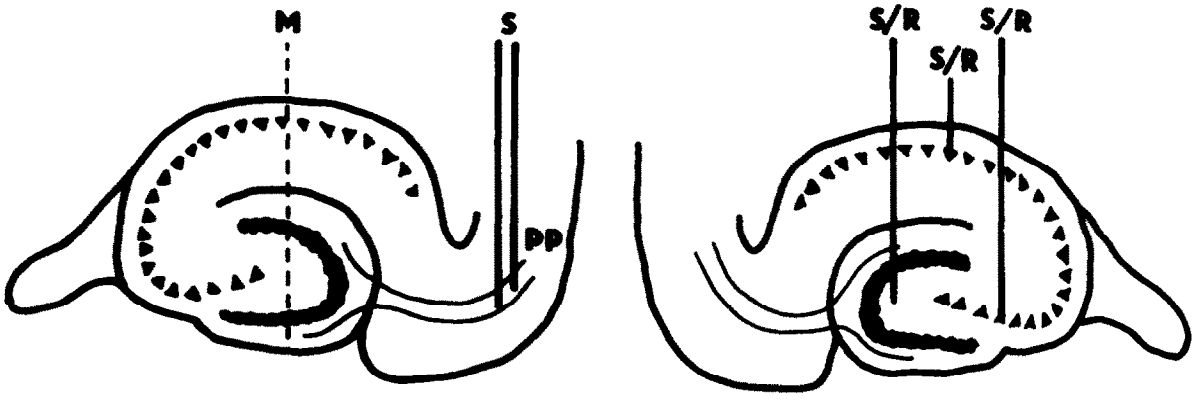

Fig. 1. Schematic section through left and right hippocampal formations showing electrode positions. PP, perforant path; S, stimulation electrode; M, recording electrode; S/R, stimulation or recording electrode.

= 4.0) and served as an indwelling lesioning electrode. A medial septum lesion was produced under light ether anesthesia by passing 2.5 mA anodal current through the implanted electrode for 20 s. A wire in the rectum served as the cathode. One week was allowed for recovery. In 3 animals the entire left hippocampus and the overlying neocortex was removed by suction. In another 3 rats a 2 mm strip of the neocortex and white matter was removed bilaterally from the midline to the rhinal fissure, 6 mm posterior to bregma. The purpose of this operation was to disconnect the entorhinal cortex from its cortical afferents[14,36,136,137]. In 4 additional animals the fimbria–fornix and the overlying neocortex was cut with a microknife (fi-fo-cx group). The cut was made in the frontal plane (AP = 1.5) and extended to cut all fibers of the fimbria–fornix system (L = ± 5.0 mm; V = 4.5). Four weeks were allowed for recovery after which these animals were implanted in the manner described above.

2.5. *Recording and stimulation*

Recordings of unit activity were made bipolarly between the roving microelectrode and the ipsilateral electrode fixed in stratum oriens or pyramidale of CA1. Between 1 and 5 tracks were made in each animal (1 track per session). A dual field effect transistor in a source follower configuration was used to eliminate movement artifact. The slow waves from the microelectrode and other recording electrodes were recorded monopolarly. The unit channel was passed through a second order active filter (0.5–10 KHz). Unitary activity and the EEG were recorded on magnetic tape and by a Grass polygraph (using a Schmitt trigger to record unit discharges). Evoked field potentials and cell discharges were monitored on a storage oscilloscope. Single stimulus pulses (0.1 msec; 15–800 μA) were applied to either the hippocampal or angular bundle stimulating electrodes. Stimulation was either bipolar or monopolar against the ground electrode with the active electrode being cathodal[26]. A signal averager (Digitimer Neurolog) was used to average field potentials, routinely 8 or 16 responses.

2.6. *Data processing*

2.6.1. *EEG*

Selected EEG segments of 5 s each were filtered between 0.5 and 100 Hz, sampled at 200 times/s and stored on a disk by a microcomputer (Cromemco System 3). Each segment was then tapered off at the ends according to a cosine function and converted into the frequency domain by Fast Fourier Transform (FFT). The transformed data were smoothed by an elliptical function across frequencies and plotted as a function of frequency (0–100 Hz). Auto-power spectra of single EEG segments and coherence and phase spectra of a pair of EEG records (reference and microelectrode) were plotted. Each spectrum was averaged from 4 to 8 EEG segments recorded during identical behavior patterns. Both linear and logarithmic power, linear and Fisher z-transform coherence were plotted[78].

2.6.2. *Unitary activity and correlation with EEG*

Window discriminated spike occurrence times were computed and stored at a resolution of 0.1 ms. Temporal firing of units in relation to EEG waves required storage of the bin address of the first spike and subsequent adjacent spike intervals, from which interval histograms were constructed. The spike interval times were also used to construct a spike train (number of firings per bin) with a bin-width equal to that of the digitized EEG (normally 5 ms). The constructed spike train was analyzed like EEG signals (above) for the calculation of spectra. Auto-power spectrum of the spike train and coherence and phase spectra of the spike train in relation to EEG were plotted.

2.6.3. *Spike triggered averaging*

In addition to spectral analysis, the temporal correlation of EEG and units was also estimated by an analog averager (Digitimer Neurolog 750) by averaging consecutive EEG samples (100 ms to 0.5 s) derived from the microelectrode and the reference electrode and using the spike as a trigger signal[23,24]. This procedure is formally similar to calculating the cross-correlation function of unit and EEG. However, following a spontaneously occurring trigger spike the second and subsequent spikes within a given sweep do not trigger averages. Despite this, the am-

plitude and phase of the spike-triggered average are good indicators of the temporal correlation of unit firing and EEG in the time domain, comparing well with coherence and phase estimates in the frequency domain. Control experiments disclosed that hippocampal slow wave averages triggered by neocortical units or random pulses were usually flat. In the present experiments between 128 and 2048 sweeps were commonly used for averaging. In some cases the slow waves were delayed (Neurolog 740) in order to better judge the phase relationship. The positive peak of the averaged waves was regarded as a phase of 90°. The computation of spike-triggered averages is much faster than spectral analysis and phase-locking of extremely slowly firing units to slow waves could be calculated by this procedure. Spontaneous unit activity was also averaged by spike triggering to construct post-firing interval distribution histograms (Fig. 3f).

2.7. *Histology*

Following the last penetration the microelectrode was left in the brain and the animals were deeply anesthetized with sodium pentobarbital. Anodal currents (5–10 μA for 10 s) were passed through the electrodes. The rats were perfused transcardially with physiological saline, 4% solution of potassium ferrocyanide (Prussian blue reaction, used to localize steel electrodes) and 10% formalin. Coronal frozen sections were cut, mounted and stained with cresyl violet.

3. RESULTS

3.1. *Classification of hippocampal units*

A total of 280 single cells were isolated and studied physiologically. Spontaneous EEG and evoked field profiles and histological reconstruction of the recording tracks allowed a precise localization of the position of the recording microelectrode. Cells were classified according to their spontaneous and evoked response properties.

About half of the isolated neurons were complex-spike cells[105]. All of them were found in the CA1 pyramidal layer and in the hilus of the dentate gyrus. The duration of the unfiltered spikes varied between 0.5 and 1.2 ms (filtered negative component 0.35–0.6 ms). Although not specifically looked for, some of the complex-spike cells discharged at a significantly higher rate in some parts of the experimental chamber than in other parts. Apart from these 'place' correlates[99,100], complex-spike cells fired at a very low rate (0.02–2.8 Hz). The highest frequency was observed when the rat was in a drowsy state (sitting still with high amplitude irregular waves present in the hippocampal EEG) followed by drinking and immobility and lowest when the rat was walking around or running. Indeed, some complex-spike cells stopped discharging altogether when the animal began to move. The majority of CA1 complex-spike cells responded to stimulation of the commissural or associational (Schaffer collaterals) inputs[25]. They always responded with a single action potential (Fig. 2A), presumably due to the operation of the recurrent inhibitory circuitry[2,9,19,25,26,44]. Thresholds were usually high and only 5 complex-spike units responded with current intensities lower than that of the threshold of the population spike. Latency of firing was a function of stimulus intensity but no complex-spike unit in the CA1 region responded earlier than 1.4 ms after the onset of the extracellularly recorded field post-synaptic potential[26]. Response characteristics of the hilar complex-spike cells were similar, although 2 cells discharged twice to commissural activation. Earlier studies revealed that the two action potentials represented antidromic and orthodromic activation of the same neuron[23]. Perforant path stimulation was able to drive complex-spike cells of the hilus only with current intensities which exceeded the threshold of the population spike. As a rule the latency of the unit response was 0.2–0.8 ms longer than the peak latency of the population spike representing granule cell discharges (Fig. 2C).

Fox and Ranck[43], on the basis of the anatomical distribution of the complex-spike cells, suggested that this class of neurons correspond to pyramidal cells. Cells with the above physiological characteristics have been described both in acute and in in vitro preparations, and have been stained with intracellular techniques[19,26,41,44,132,145]. Consequently, the evidence is strong that complex-spike cells are indeed pyramidal cells.

Granule cells are the other principal cell type in the hippocampal formation. No physiological criteria have yet been adopted for the classification of gran-

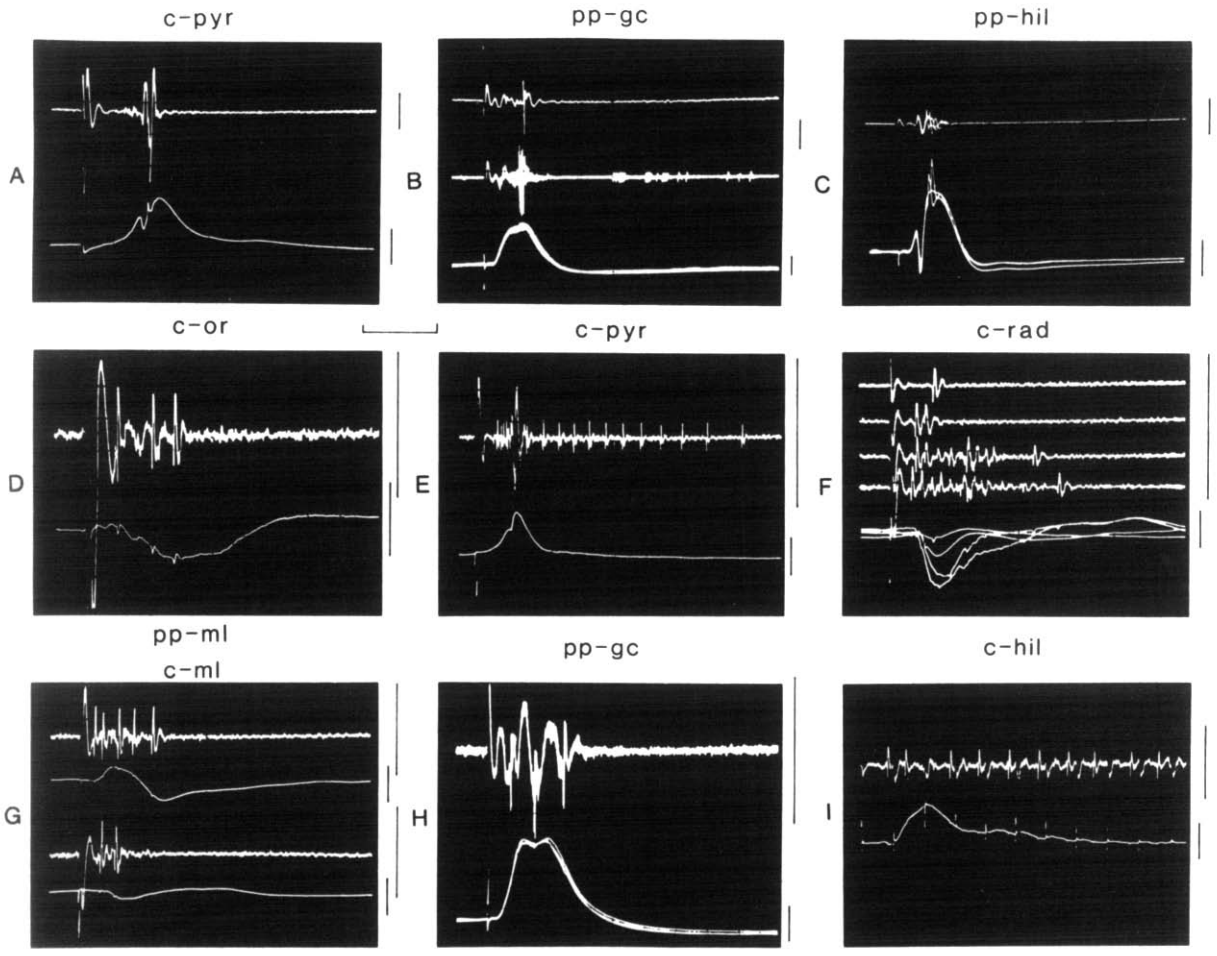

Fig. 2. Evoked response properties of hippocampal neurons. Upper trace is filtered (0.5–10 KHz), lower trace is wide band (1 Hz–3 KHz). A: CA1 complex-spike cells; discharge in response to stimulation of the commissural path (C) at 20% above spike threshold (T) (1.2 T). B: granule cell; 1.3 T. Upper trace: single sweep. Middle and lower traces: 10 superimposed sweeps. The small unit is presumably a basket neuron in the granule cell layer. C: disynaptically[121,122] activated complex-spike cell in the hilus; 1.0 T; 3 sweeps. Note the presence of a high amplitude population spike. D, E and F: interneurons in strata oriens (1.2 T), pyramidale (2.5 T) and radiatum (1.0, 1.1, 1.8 and 2.1 T) of CA1, respectively. G, H and I: interneurons in the molecular layer (1.3 T and 1.1 T), granule cell layer (1.4 T; 3 sweeps) and hilus (1.2 T) of the dentate gyrus, respectively. Note high frequency following (200 Hz) and latency jitter in I. Abbreviations above panels indicate stimulated and recording sites, respectively. c, commissural path; pp, perforant path; pyr, CA1 pyramidal layer; gc, granule cell layer; hil, hilus; or, stratum oriens of CA1; rad, stratum radiatum of CA1; ml, molecular layer. Calibrations: 10 ms (A, B, C, D, E, G, I), 20 ms (E); 5 mV (field A, B, C, E, G, H, I), 1 mV (field D, F), 30 μV (unit A, B, D, E, F, G, H, I), 5 mV (unit C). Positivity up.

ule cells. Short latency firing to perforant path stimulation alone[19] (3–5 ms) is clearly not sufficient since basket cells of the granule cell layer[109,116] and hilar cells with dendrites in the molecular layer[1,110] may respond with similar latency[23,26]. In the present study the following criteria were used to tentatively identify granule cells. (1) The unit had to be located within 330 μm (1 turn of the microdrive) following the reversal of the perforant path field response, i.e., in the granule cell layer. Identification of the cell layer was aided by the presence of multiple unit discharges firing in synchrony with the simultaneously recorded rhythmic slow waves (see below). (2) The isolated unit responded only once to either commissural or perforant path stimulation. This criterion is based on the finding that perforant path stimulation never evokes multiple population spikes, presumably because of strong recurrent inhibition[2,5,9,10,19,26,80]. (3) In response to strong stimulation of the perforant path, evoking a large population spike, the unit

should not fire on the falling part of the positive wave following the population spike. The practical constraint of the second criterion was the difficulty of isolating single cells since granule cells are so closely packed. In several instances perforant path stimulation resulted in 'repetitive' unit discharges. Repeated observations revealed, however, that single discharges of several units of different amplitude, rather than repetitive discharge of a single cell, contributed to the 'multiple' response. Due to these difficulties only 29 units could be tentatively classified as granule cells (Fig. 2B). Cells with features (1)–(3) differed considerably from pyramidal cells. They never showed complex spike patterns. Duration of the spikes varied between 0.22 and 0.40 ms (negative component; filtered). They were able to follow orthodromic activation of the perforant path up to 80 Hz.

The third main cell population of the hippocampal formation consists of local circuit neurons or interneurons*. Most prevalent among the interneurons are the basket cells[17,52,83,104,107,109,117,118]. Their suggested functional role is inhibition[2,3,8,9,66,120]. Indeed, nearly all interneurons in CA1 and the dentate gyrus contain glutamic acid decarboxylase (GAD)[110,118] the synthesizing enzyme for the inhibitory neurotransmitter, GABA[33]. In agreement with their anatomical distribution[52,83,104,110,112,118] the overwhelming majority of interneurons were found in strata oriens and pyramidale of CA1 and the hilus of the dentate gyrus. Despite their marked morphological variation[109,110,117,118], electrophysiological properties of the interneurons appeared very similar. In agreement with previous reports[8,9,24,26,37,44,114] the spike duration of interneurons was short (0.23–0.44 ms, negative component, filtered), their discharge rate was high (5–70 Hz) and varied with behavior in a predictable manner. The most stringent physiological criterion of an interneuron is its repetitive and high frequency discharge in response to afferent excitation[2,9,13,19,24,26,37,40,44,114,132]. The number of repetitive discharges is a function of stimulus intensity[2,26,40,44]. Neurons with these features have been described both in in vivo and in vitro preparations and were identified as interneurons by intracellular dye injections[9,13,26,40,68,114,132].

The threshold of 74% of the interneurons was below the threshold of the population spike. Five interneurons (4 in CA1 region, 1 in the dentate gyrus) responded reliably to 15 μA stimulus current, at which intensity no field responses were present. Sixty-eight percent of the interneurons had latencies shorter than the onset of the respective population spike. Indeed, some of them fired earlier or coincided with the onset of the extracellularly recorded post-synaptic potential (Fig. 2D, F, G and I). They were able to follow high frequency (up to 200 Hz) trains of orthodromic volleys (Fig. 2I). Interneurons had obvious behavioral correlates (see below) except for 3 constant firing neurons[105]. These latter units (1 in CA1, 2 in hilus) fired at a fairly constant frequency (40–60 Hz) independent of overt behavior.

In the present study a hitherto undescribed cell type was observed in the hilus. This unit (n = 3) fired at a regular rate of about 15–25 Hz when the animal was drinking, grooming, or stayed motionless, but virtually stopped responding whenever the rat began to move and RSA occurred in the hippocampal record. Therefore we called them 'antitheta' cells.

In addition to the above groups of neurons several other units were isolated but were not held long enough to examine their physiological characteristics and could not be classified in any of the above cell types. These units will not be dealt with further.

3.2. *RSA and single cell activity*

3.2.1. *Intact animals*

Since RSA showed a gradual phase shift as the microelectrode penetrated the different anatomical strata (see below), the phase relationship between unitary activity and slow waves was always compared with both the locally derived EEG and slow waves derived from a fixed reference electrode. Pilot studies indicated that the morphological aspects and coherence of the slow waves above the pyramidal layer were quite similar up to the level of the corpus callosum in contrast to the 'deep' RSA derived from below the pyramidal layer. Therefore the less variable RSA recorded from the stratum oriens or pyramidale was used as a reference.

Interneurons showed an obvious relationship with

* In light of recent findings neither anatomical term is precise since at least some of the GAD-containing neurons do project out of the hippocampus[22,31,118].

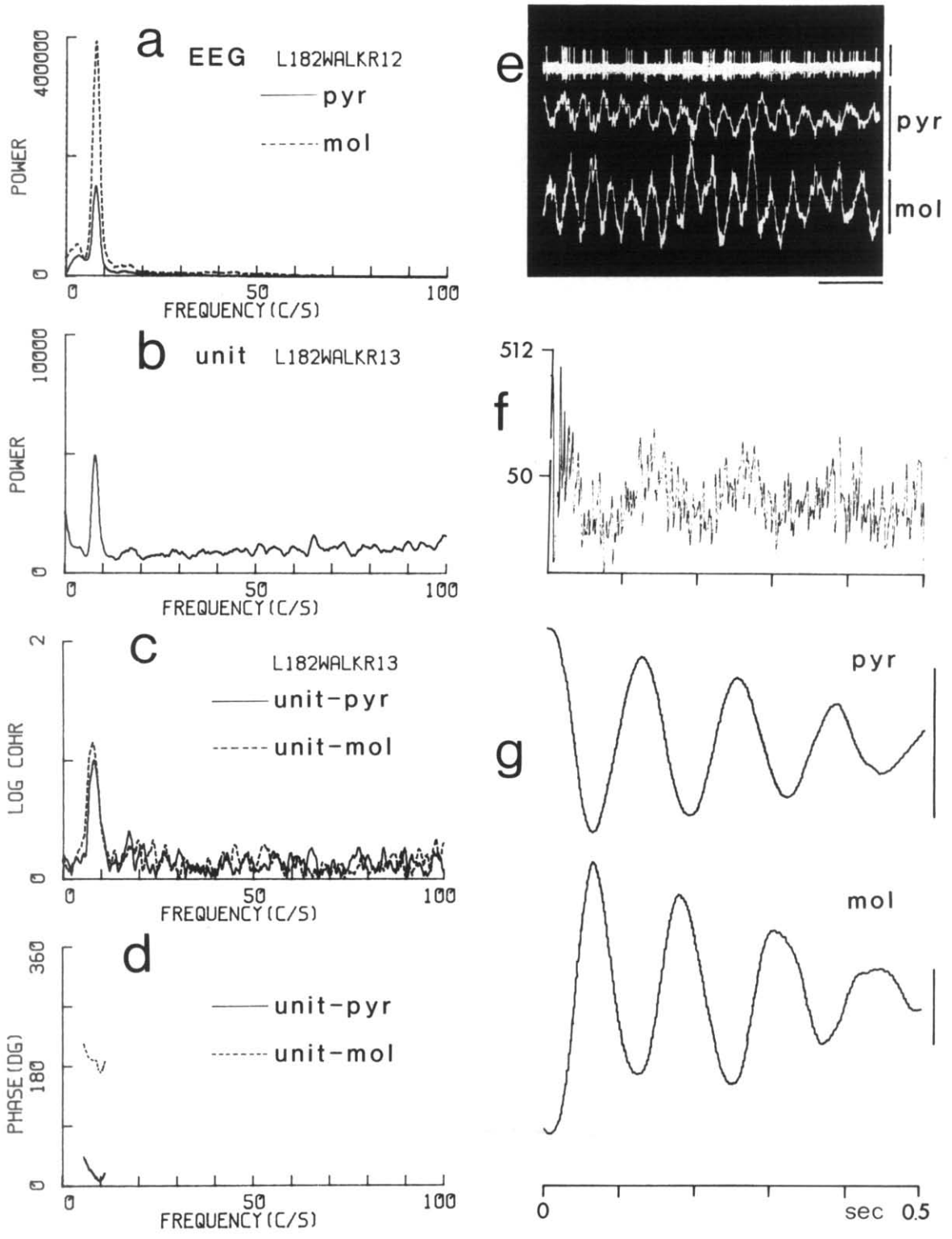

Fig. 3. Relationship between firing pattern of a CA1 pyramidal layer interneuron and RSA in the frequency domain (a–d) and time domain (e–g) during walking. a: power spectra of EEG derived from the microelectrode (pyr) and a fixed reference electrode in the dentate molecular layer (mol). b: power spectrum of unit firing. c: z-transform coherence spectra between unitary activity and EEG. d: phase spectra between unit activity and EEG at RSA frequency with high coherence values. e: relationship between unit activity and

the concurrent EEG. Whenever RSA appeared in the hippocampal record, cells of this class increased their firing rates[100,105,111]. There was a positive relationship between RSA frequency and the number of unit discharges during a given slow wave cycle. The average number of spikes during a given frequency of RSA varied from cell to cell. The highest level was observed in the interneurons of the stratum oriens of CA1 (5–15 spikes per theta cycle) followed by stratum radiatum (4–10 spikes per cycle). Interneurons in the pyramidal layer were somewhat slower (3–8 spikes per cycle). Interneurons in the dentate gyrus were quite variable. Some cells were comparable to stratum oriens neurons, some discharged only 1 or 2 spikes per theta cycle. The rhythmicity of discharges correlated well with the ongoing EEG as revealed by the power spectra of the cell discharges as a function of frequency as well as by the high coherence values between unitary activity and slow waves in the theta band (Fig. 3). Occasionally, a second harmonic component at twice the RSA frequency was also present in the unit power spectrum. The RSA rhythmicity was also shown by the post-firing interval distribution histograms in the time domain (Fig. 3f).

Interneurons in strata oriens and pyramidale began firing during the positive peak of their locally derived RSA waves. In most instances this was obvious by visual inspection, in other cases this correlation could be revealed by either the spectral or the spike triggered averaging methods (Fig. 3). Four out of 5 interneurons found in the stratum radiatum of CA1 also fired preferentially on the positive portion of the theta waves derived from the reference electrode, although their relationship to the local waves varied as a function of distance from the pyramidal layer. That is, they fired in synchrony with the majority of stratum oriens/pyramidale interneurons.

A small portion of the dentate hilus interneurons also discharged during the positive peak of the reference theta waves. The majority of them, however, fired mainly on the positive portion of their locally derived RSA which corresponded to the falling portion (150–240°) of the reference RSA waves (Fig. 4).

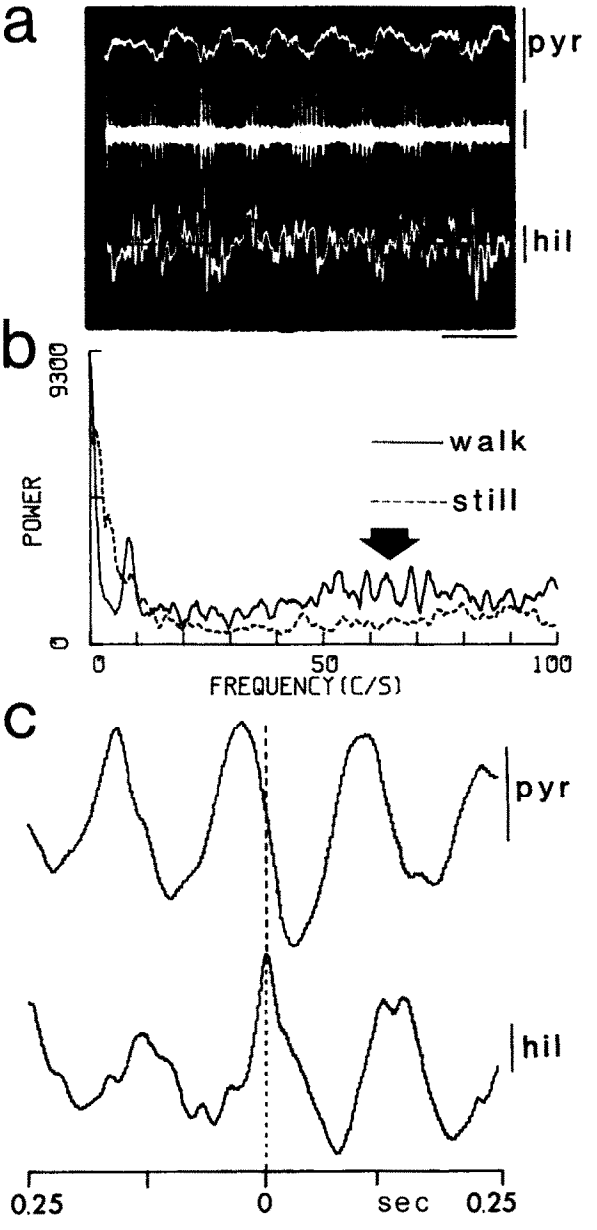

Fig. 4. Interneuron in the hilus of the dentate gyrus. a: unit firing and simultaneous slow waves from a fixed reference electrode in the CA1 pyramidal layer (upper) and from the microelectrode (lower) during walking. b: power spectrum of cellular activity during walking (walk) and immobility (still). Note absence of peak in the RSA band and decrease in fast activity (arrow) during immobility. c: spike-triggered averages of slow waves (1–30 Hz); 256 repetitions. Spike occurrence is at 0 s. Calibrations: a — 20 μV (unit), 1 mV (EEG), 0.2 s; c — 100 μV. Positivity up.

slow waves. f: post-firing interval distribution histogram; 512 repetitions. g: spike-triggered averages of slow waves (1–30 Hz); 512 repetitions. In f and g the averager was triggered by spontaneous unit discharges. Note phase relationship between unit and EEG (d–g). Note also peaks in the RSA band in a–c. Calibrations: e — 20 μV (unit), 1 mV (EEG), 0.2 s; g — 100 μV. Positivity up.

Description of discharge patterns of the granule cells is based on the isolated single units as well as on their population behavior. With low impedance electrodes (≤ 3 MΩ) the activity of several granule cells could be simultaneously recorded when the microelectrode approached the granule cell layer. Similarly to complex-spike cells, the putative granule cells showed higher frequency discharges in the drowsy state than during drinking and immobility. However, in contrast to complex-spike cells, granule cells considerably increased their firing rate whenever the rat began to move about and RSA appeared in the hippocampal record[111]. The frequency of the multiple unit discharge increased periodically with each theta cycle. The peak of the envelope of multiple unit activity coincided with the positive peak of the locally derived theta waves (Fig. 5a). This consistent population pattern of granule cells was an easy and important method of identifying the granule cell layer[19], and was found at both the ectal and endal blades, but not in the hilus. Single unit activity essentially confirmed our observations on the population pattern (Fig. 5). Thus, behavioral correlates of granule cells was similar to those of the interneurons, although differences were also noted. The most notable difference was the very wide dynamic range of the firing rate of granule cells across different behaviors. Some of them fired at a very low rate when the rat was sitting immobile but alert (1–4 Hz). During running the frequency could increase up to 80 Hz. In contrast to interneurons, the relationship between unit firing and slow waves was hard to assess by visual inspection. However, the power density histogram and spike-triggered averaging always revealed regularity in the RSA band (Fig. 5c, d).

In the CA1 region the population behavior of complex-spike cells was studied by multiple unit recording. Multiple unit discharges were periodically suppressed at the positive peak of the locally derived theta waves (Fig. 6a). This population behavior was

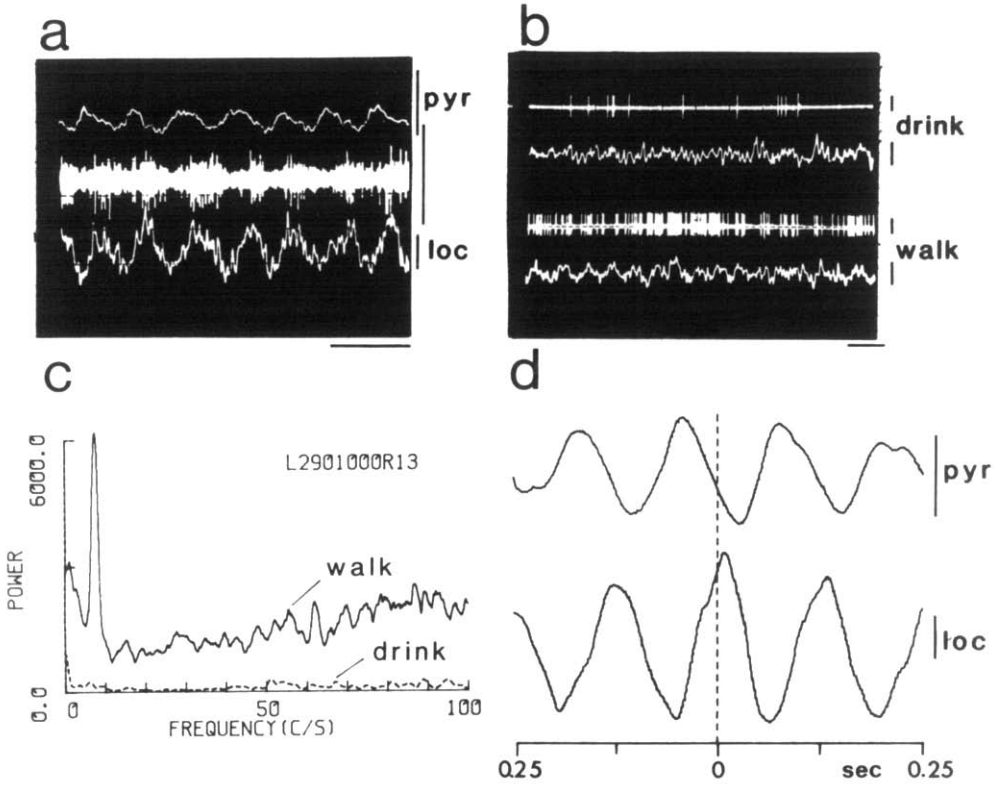

Fig. 5. a: multiple-unit activity in the granule cell layer. pyr, reference electrode in CA1 pyramidal layer; loc, microelectrode. Note rhythmic activity of the granule cells and phase-relationship with slow waves. b: patterns of isolated granule cell during drinking and walking. c: power spectra of the unit shown in b. Note peak in RSA band during walking. d: spike-triggered averages of slow waves (1–30 Hz); 256 repetitions. Calibrations: a, b — 10 μV (unit), 1 mV (EEG), 0.2 s; d — 100 μV. Positivity up.

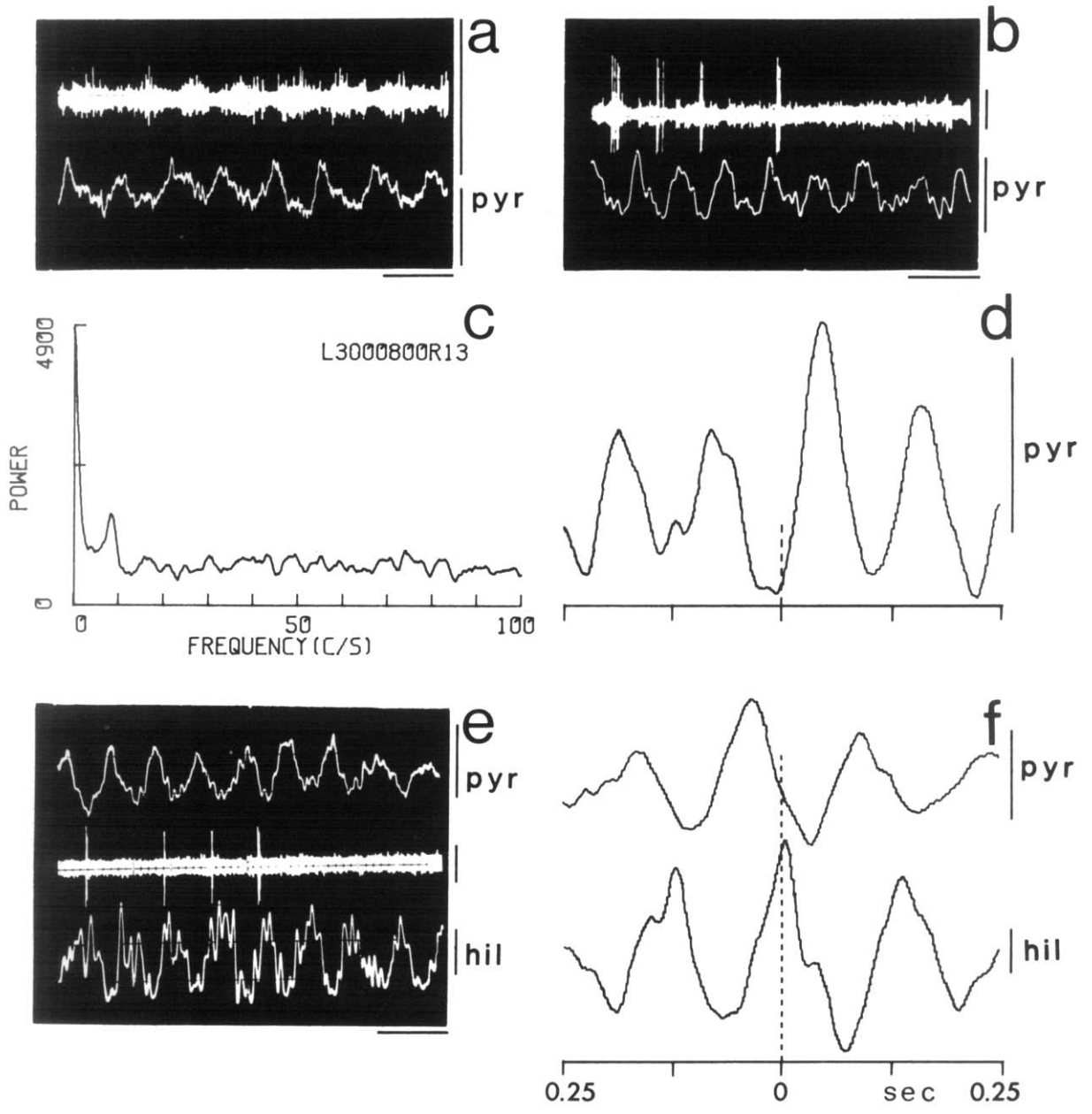

Fig. 6. Complex-spike cells in CA1 (a–d) and in the hilus (e and f). a: multiple-unit activity and EEG in the CA1 pyramidal layer (pyr). Note suppression of cell discharges during the positive peaks of RSA waves. b: isolated CA1 complex-spike cell. c: power spectrum of the cell shown in b obtained while the animal was walking and rearing in the 'spatial field' of the cell[99]. This cell showed the highest peak in the RSA band of all complex-spike cells. d: spike-triggered average of the locally derived EEG (1–30 Hz); 256 repetitions. e: complex-spike cell in the hilus (hil) while the rat crossed the 'spatial field' of the cell. f: spike-triggered averages of EEG (1–30 Hz) triggered by the cell shown in e during walking. Calibrations: a, b, e — 20 μV (unit), 1 mV (EEG), 0.2 s; d and f — 100 μV. Positivity up.

also frequently observed in the high-pass filtered record of the fixed reference electrode placed in the CA1 pyramidal layer. Isolated single complex-spike cells, in general, showed no apparent rhythmicity and had a very low discharge rate during the presence of hippocampal RSA (0.01–1.7 Hz). Exceptions to this rule occurred when the animal was moving in the 'spatial field' of the unit[99,100]. In these in-

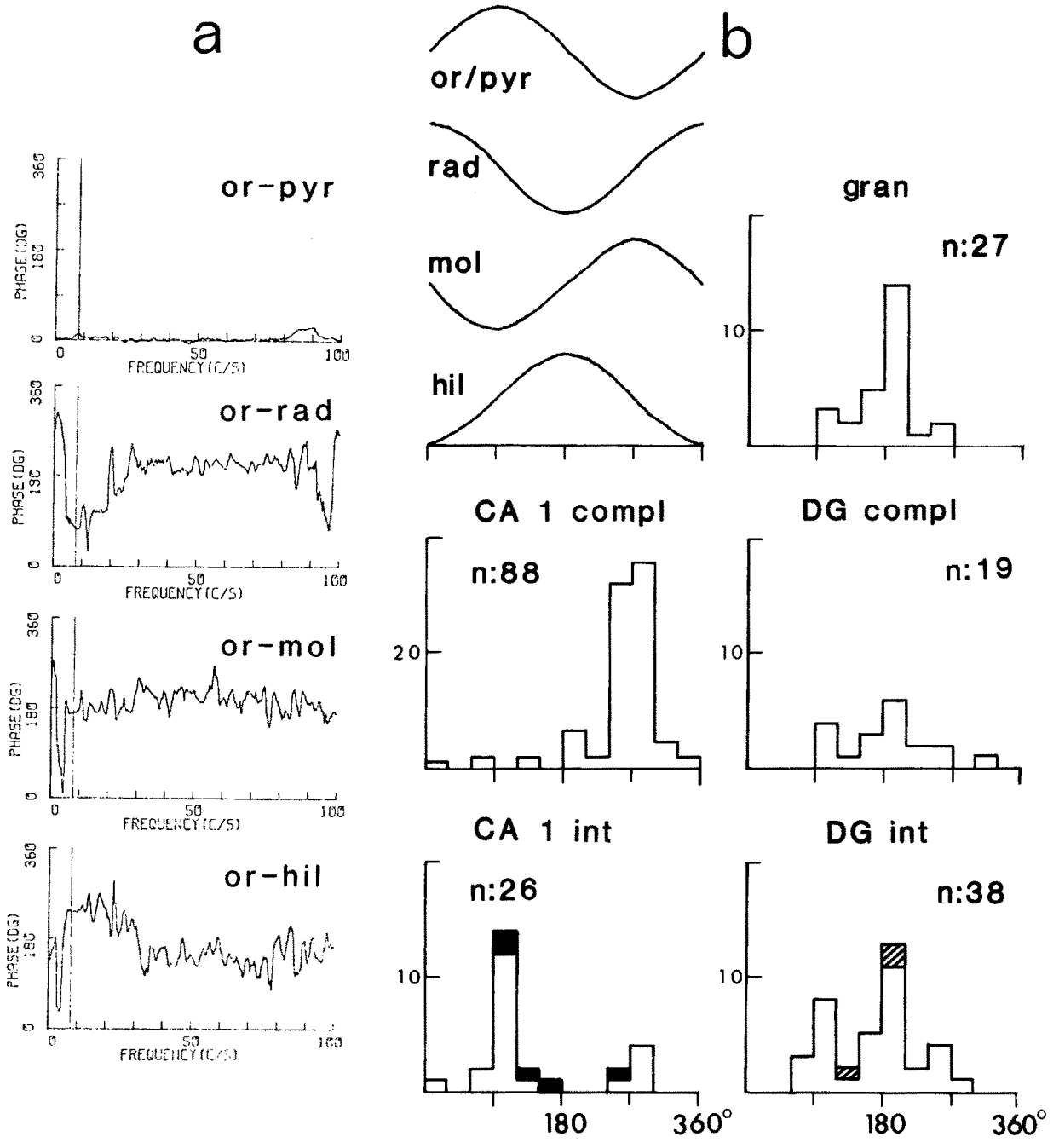

Fig. 7. a: phase spectra between pairs of EEG recorded from a reference electrode in stratum oriens of CA1 (or) and the microelectrode at 4 different depths. The vertical line indicates the peak of power in the RSA band (not shown). pyr, CA1 pyramidal layer; rad, stratum radiatum of CA1; mol, molecular layer of the dentate gyrus; hil, hilus. Note abrupt phase-reversal of fast activity when the electrode moved into the stratum radiatum. Note also phase-shifts between pyramidal layer and radiatum, and molecular layer and hilus in the RSA band. b: phase-relation of various cell types to the reference RSA in CA1 pyramidal layer. Phase-relationship of RSA waves at different depths are shown schematically. Black columns: interneurons (int) in stratum radiatum. Cross hatched columns: interneurons in molecular layer of the dentate gyrus (DG). Note opposite phase-relationship of complex-spike cells (compl) and interneurons in CA1 and synchrony of granule cells (gran), complex-spike cells and interneurons in the dentate gyrus. Note also about 90° delay of CA1 complex-spike cells relative to dentate neurons.

stances its frequency could increase up to 7–12 Hz, often in a rhythmic manner with the slow waves (Fig. 6b). Only under these circumstances did the power spectrum of the unit show moderate dominance at theta frequency (Fig. 6c). Complex-spike cells in the CA1 region fired preferentially on the negative portion of the locally derived RSA waves (Fig. 6d). The behavior of the complex-spike cells in the hilus was essentially similar. However, they discharged mainly on the positive phase of the local RSA[143] or on the falling portion of the reference RSA waves (Fig. 6e, f).

In order to assess the phase relationships between the different cell groups, and between the unit activity and hippocampal RSA, the histograms of Fig. 7 show the phase relation of all units in reference to the fixed electrode placed in the pyramidal layer of CA1. Also shown in the figure is the theta wave profile in different depths of the hippocampal formation. Random relationship between the single unit discharge probability and the phase of theta could be rejected in all cell groups ($P < 0.05$, chi-square). In the CA1 region complex-spike cells and interneurons fired on opposite phases of the theta waves. In the dentate gyrus all cells appeared to fire in synchrony about 90° before the CA1 complex-spike cells. The only exception was a small portion of dentate interneurons which fired in synchrony with the CA1 interneurons.

3.2.2. *Effect of urethane on hippocampal interneurons*

Atropine-resistant RSA present during walking can be blocked by urethane anesthesia[70,134]. In a urethane-anesthetized preparation RSA can be induced by eserine or sensory stimulation and can be blocked by cholinolytics[58,59,70,102,125,134]. Since the RSA in the walking and anesthetized animals differ in many aspects, it was important to examine the effect of urethane anesthesia at the neuronal level. Indeed, Fox et al.[45] found different phase-relationships between interneuronal activity and RSA in separate groups of undrugged and anesthetized animals and explained the difference by the blockade of the recurrent circuitry by urethane. We set out to examine the effect of urethane on the same isolated single cells after data has been collected in the behaving animal. Urethane was given intraperitoneally at a dose of 1.5 g/kg. The spontaneous and evoked discharges of the unit were continuously monitored. RSA was evoked either by pinching the tail or by lifting up the rat. We succeeded in maintaining 15 interneurons (6 in CA1, 9 in the dentate gyrus).

Following urethane anesthesia the average frequency of cell discharge decreased, sometimes as much as 50%. Coherence with slow waves and rhythmicity of firing also decreased, although the unit power spectra still showed a peak at theta frequency (Fig. 8). Despite these changes interneurons retained their phase-relationships with RSA. Fig. 9 summarizes the data obtained on all cells. Only one interneuron in the stratum radiatum of CA1 showed an apparent phase-reversal with respect to the locally derived RSA. However, the phase-relationship of the same neuron to the reference RSA did not change. The phase-relationship between slow waves derived from the microelectrode and reference electrode shifted in a similar manner indicating that the apparent phase-shift of this neuron was a consequence of the different RSA depth profiles in the awake and anesthetized animal[141].

3.2.3. *Effect of atropine on neuronal activity*

We examined the effect of atropine on 9 interneurons (5 in CA1, 4 in dentate gyrus). Atropine was given intraperitoneally at a dose of 50 mg/kg. The drug abolished the RSA normally present during small head movements, but RSA accompanying rearing, walking and running was clearly preserved. Atropine increased the rat's tendency to run in the wheel even after satiation and this was further facilitated by turning off the room lights. All 9 interneurons preserved their phase-correlation with slow waves. Other aspects of neuronal firing were altered, however. It was frequently observed that the cell occasionally stopped firing for 2–5 theta cycles and then resumed its rhythmic discharge pattern again (Fig. 10a). This point requires emphasis since such 'failures' very rarely occurred in the undrugged animal during running. In 6 out of the 9 cases the power of unit firing in the theta band decreased, although slow wave power remained unchanged or even slightly increased. Further, the power in the low frequency band (1–6 Hz) increased both in the unit and EEG spectra. The spike 'failures' during theta cycles were quantitatively reflected by the decrease of the coherence between unit activity and RSA (Fig. 10e),

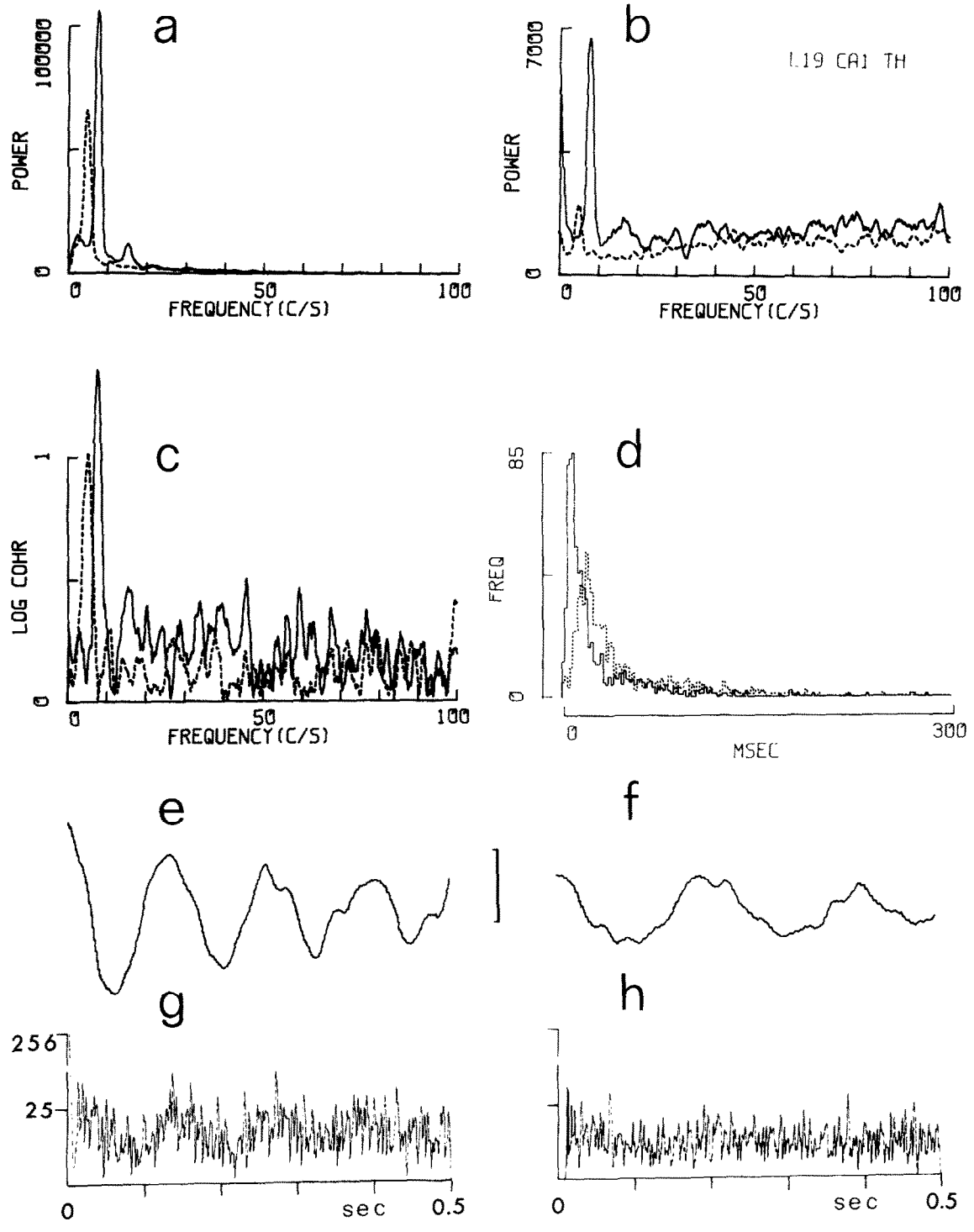

Fig. 8. Effect of urethane on interneuronal activity and EEG. a: EEG spectra recorded from the microelectrode in CA1 pyramidal layer during walking (solid line) and during urethane anesthesia (discontinuous line). b: power spectra of unitary activity. c: z-transform coherence spectra between EEG and unit activity. d: interspike-interval histograms. e, f: spike-triggered averages of EEG before (e) and after (f) urethane (1–30 Hz). g, h: post-firing interval distribution histograms before (g) and after (h) urethane; 256 repetitions (e–h). Note unchanged phase-relation between unit activity and RSA (e and f) and downward shifts of spectral peaks (a–c). Calibration: 100 μV (e and f). Positivity up.

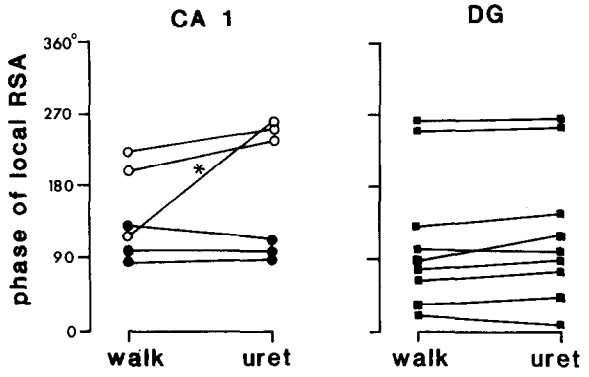

Fig. 9. Phase-relationship between interneuronal activity and locally recorded RSA during walking (walk) and urethane anesthesia (uret). Empty circles: interneurons in stratum radiatum of CA1. Black circles: interneurons in stratum pyramidale of CA1. Black squares: interneurons in the dentate gyrus (DG). Note similar phase relationship during walking and anesthesia. The interneuron marked by asterisk showed less than 30° phase-shifts when compared to the pyramidal layer reference electrode RSA.

which was observed in all animals.

Although the effect of atropine was not investigated on the *same* complex-spike cell, we observed that the frequency of firing of complex-spike cells generally increased following atropine administration. Four out of 17 isolated cells showed an average firing rate of higher than 2.4 Hz during walking. Such high frequency activity was never observed in the undrugged rat[100,105].

3.2.4. *Entorhinal cortex isolation*

Vanderwolf and Leung[135,136] reported that following bilateral lesions of the entorhinal cortex or after isolating the posterior part of the cortex from its rostral cortical connections, atropine or scopolamine would abolish all RSA from the hippocampus. The present experiments confirmed their findings. In all 3 rats the lesion removed all gray matter and white

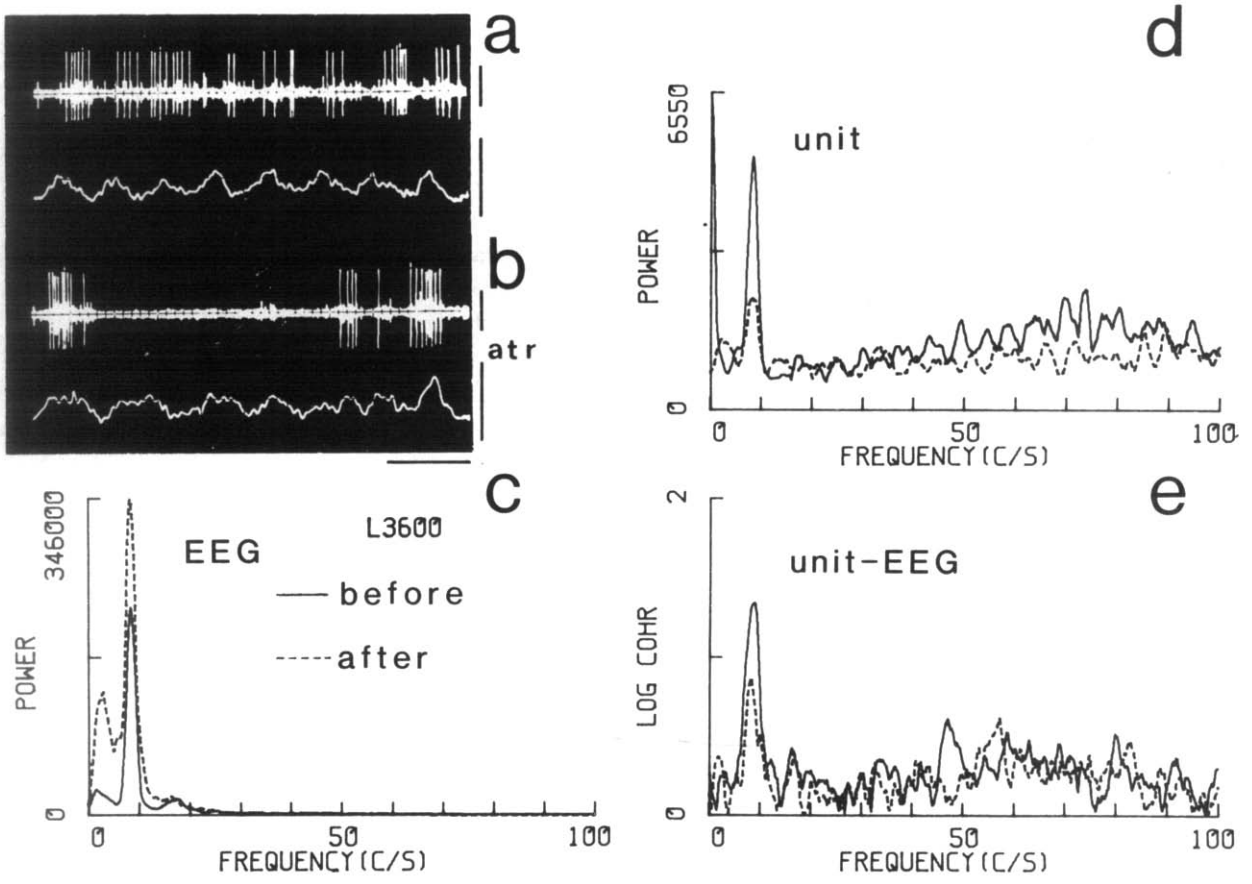

Fig. 10. Effect of atropine on interneuronal activity and EEG. a, b: activity of a CA1 interneuron in relation to locally derived EEG during walking before (a) and after (b) atropine administration. Note spike failures in b. c–e: power spectra of EEG (c) and unit activity (d) and z-transform coherence spectra between unit firing and EEG (e) before and after atropine. Note decrease of spectral peaks in d and e and concurrent increase of EEG power in c. Calibrations: 20 μV (unit), 1 mV (EEG), 0.2 s.

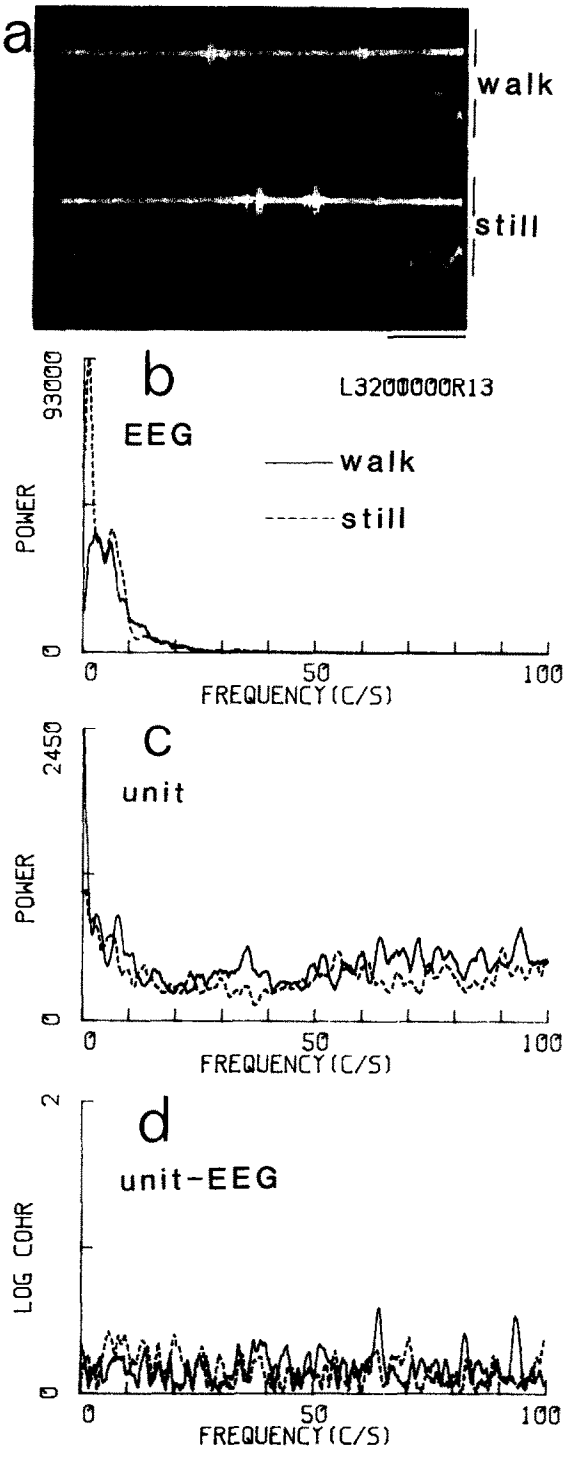

Fig. 11. Effect of atropine on unit activity and EEG in a rat with entorhinal cortex isolation. a: cell firing (interneuron in hilus) and locally derived EEG during walking (walk) and immobility (still). b–d: power spectra of EEG (b) and unit activity (c), and z-transform coherence spectra between unit firing and EEG (d). Note lack of spectral peaks in the RSA band and lack of dependence on behavior.

matter including the corpus callosum in a 2–3 mm strip from the midline to the rhinal fissure. The subiculum and the ventral portion of the hippocampus was slightly damaged bilaterally in two animals. In the third animal the entire hippocampus appeared intact. RSA appeared normal in all aspects following such entorhinal cortex deafferentation in the undrugged animal. Similarly, neurons recorded from these animals did not differ from those in normal animals. RSA disappeared completely following atropine administration. Parallel with the disappearance of RSA, rhythmic firing of interneurons also ceased and was replaced by irregular bursts of discharges. It was no longer possible to predict the movement of the rat from either the EEG or unitary activity (Fig. 11).

3.2.5. *Subcortical input deafferentation*

In 8 of the 9 rats implanted with indwelling lesion electrodes in the septum, RSA was completely and bilaterally abolished after electrolytic lesions. In 5 rats both the medial and lateral nuclei were destroyed. In 2 rats only the triangular nucleus, the fornix and the ventral hippocampal commissure sustained damage, and RSA persisted in one of them. In the remaining 2 rats damage was restricted to the medial septal nucleus. In the fi–fo–cx group the fimbria–fornix complex and the overlying neocortex was completely sectioned. Some slight damage to the thalamus and the caudate nucleus was observed in all 4 rats.

Following a septal lesion, the rhythmic discharges of the interneurons were no longer present. The peak of the unit power spectrum shifted to 1–2 Hz. Unexpectedly, however, granule cells and interneurons in the dentate gyrus still consistently increased their rate of firing whenever the animal moved[111] (Fig. 12a, b) even though firing was not rhythmic. Complex-spike cells did not appear to change appreciably. In fi–fo–cx rats RSA was no longer present. Instead sharp waves dominated the hippocampal record even during running or vigorous struggling (see below). Interneurons fired in irregular bursts without any relation to behavior (Figs. 12c, d and 17). Four out of the 11 isolated interneurons were constant firing cells, a proportion which is significantly higher than in normal animals ($P < .01$). The mean firing rate of complex-spike cells during movement varied

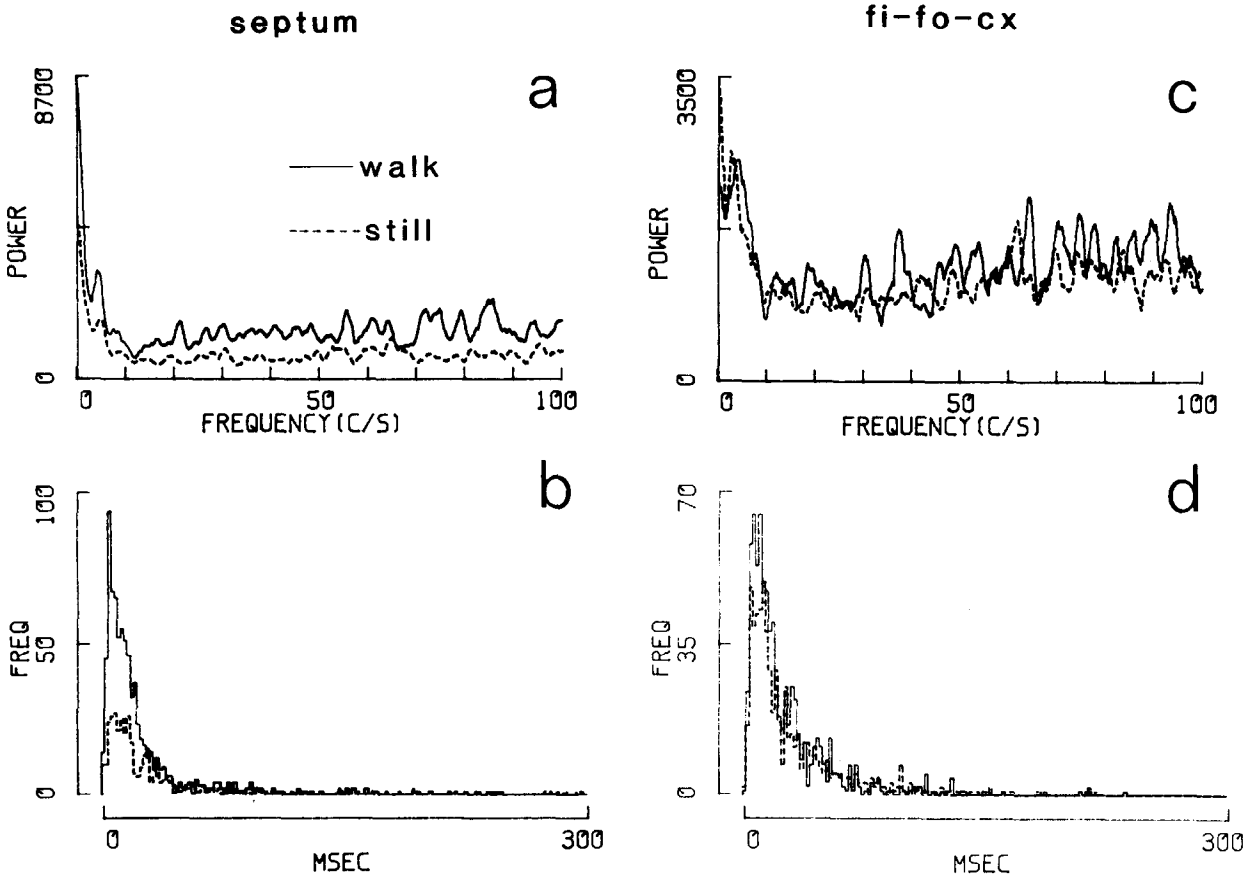

Fig. 12. Interneuronal activity in rats with septum lesion (a, b) and fi–fo–cx cut (c, d). a, c: power spectra of cellular activity (interneurons in hilus). b, d: interspike-interval histograms. Note increase in firing rate during walking in the septal animal (a, b) and the little effect of behavior on unit activity in the fi–fo–cx rat. Note also the lack of spectral peaks in the RSA band.

from the normal level (< 0.5 Hz) up to 4 Hz. A similar 3–5-fold increase in the firing rate of complex-spikes cells following fimbria–fornix lesion was reported also by Miller and Best[93].

3.3. *Large-amplitude irregular activity (LIA)*

Another characteristic slow-wave pattern which can be recorded from the rat hippocampus is an irregularly occurring sharp wave (SPW) of 40–100 ms duration[100,126,133]. This EEG pattern never occurs during behaviors accompanied by RSA. SPWs must be distinguished from large amplitude slow waves which occur in a drowsy animal or during slow wave sleep, often mixed with SPWs. Our investigation was restricted to SPWs occurring during drinking, quiet sitting and grooming.

During these behaviors SPWs occurred either in isolation or in groups of 2–7 in either a crescendo or decrescendo pattern. They occurred most frequently during drinking, followed by sitting still, face washing and fur grooming, in that order. They were easily recorded with both macroelectrodes and microelectrodes. The amplitude of a SPW was sometimes as great as 3.5 mV, but both polarity and amplitude varied as a function of the electrode location in the hippocampus (see below). SPWs occurred synchronously in both hippocampi. Microelectrode recordings revealed that SPWs were invariably correlated with the following cellular events. When the electrode penetrated the pyramidal layer, bursts of several complex-spike cells coincided with the positive going SPWs recorded with the same electrode. This bursting pattern was easily observed with relatively low impedance electrodes (< 3 MΩ) and also with the fixed reference electrode placed in the pyramidal lay-

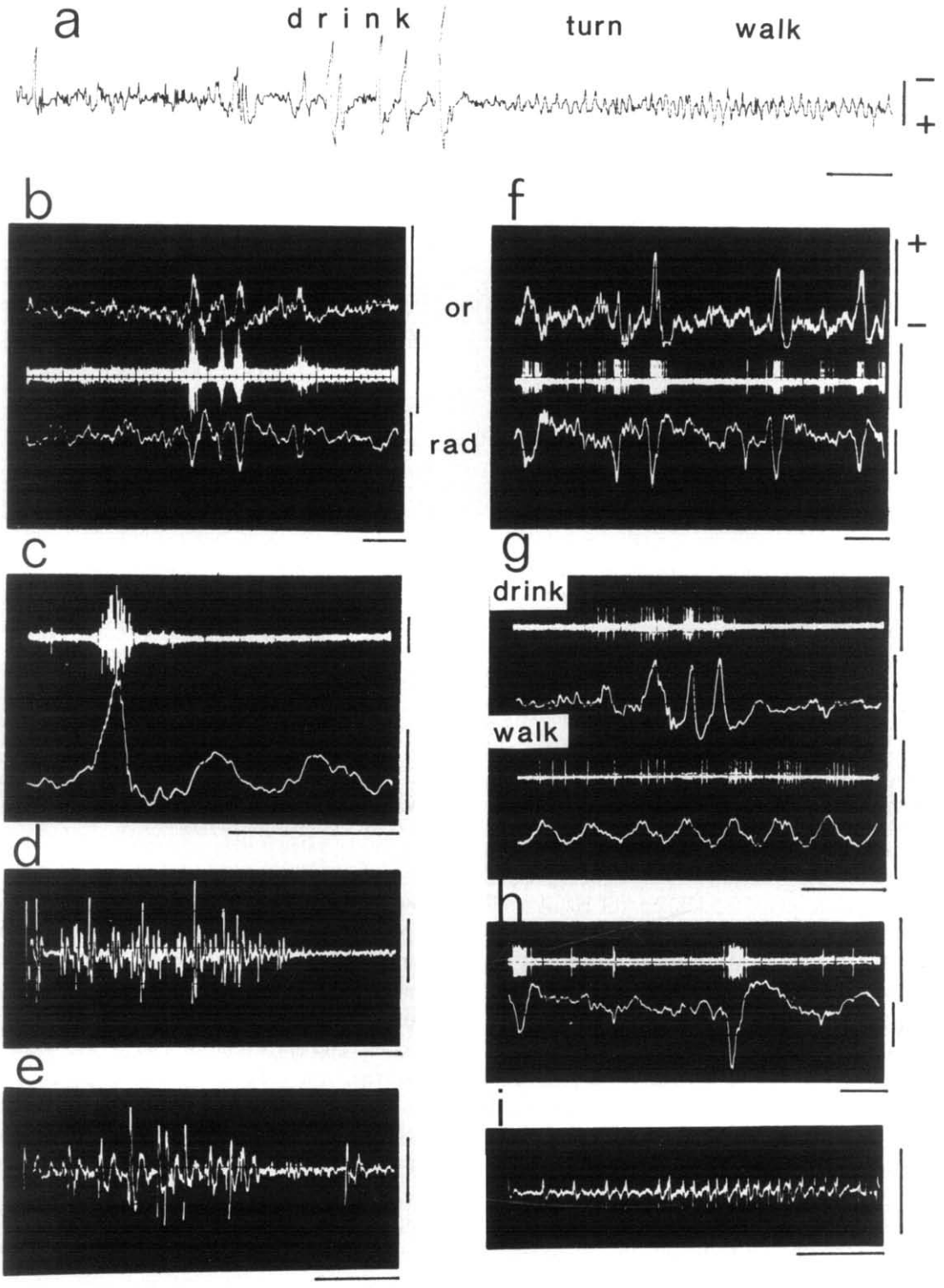

Fig. 13. Relationship between sharp waves (SPW) and cellular activity. a: EEG recorded from stratum radiatum of CA1 during drink–turn–walk transitions. Note the presence of sharp waves only during drinking. b: multiple unit activity in CA1 pyramidal layer during SPWs recorded with fixed electrodes in strata oriens (or) and radiatum of CA1. c: SPWs and concurrent burst of complex-spike cells in CA1 pyramidal layer recorded with the same microelectrode. d, e: details of multiple complex-spike bursts with faster sweeps. f: interneuron in stratum oriens of CA1. g: interneuron in the CA1 pyramidal layer. Note bursting discharges on the positive phases of

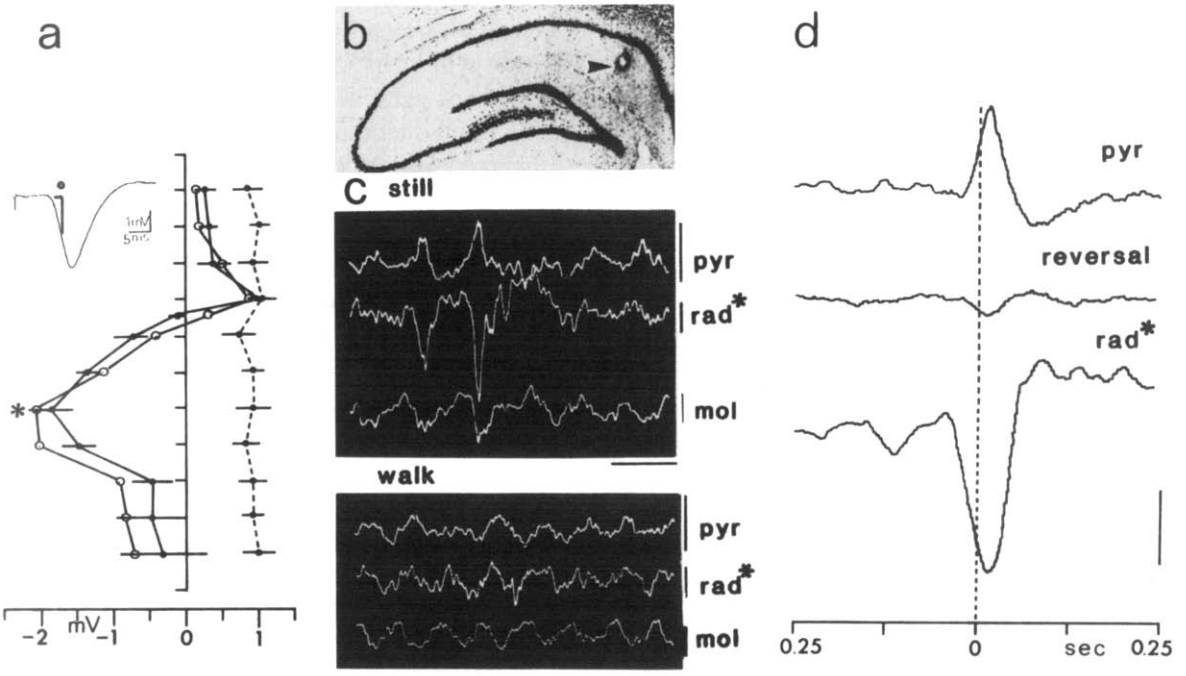

Fig. 14. a: depth-profiles of SPWs (filled circles) derived from the microelectrode (solid line) and a reference electrode in CA1 pyramidal layer (discontinuous line). Each point is an average of 30 SPWs recorded concurrently with the two electrodes. Horizontal bars indicate standard error of the mean. Also shown is the amplitude profile of the simultaneously recorded field potential evoked by stimulation of the Schaffer collaterals[25] (empty circles). Ordinate: 166 μm intervals. b: arrow indicates the position of maximum negativity of SPWs marked by an asterisk in a, c and d. c: simultaneously recorded slow waves from strata pyramidale (pyr) and radiatum (rad) of CA1 and molecular layer of the dentate gyrus (mol) during immobility (still) and walking (walk). Note polarity reversal of SPWs and gradual phase-shift of RSA. d: spike-triggered averages of SPWs from different depths (1–30 Hz). The averager was triggered by the multiple complex-spike burst recorded from a stationary reference electrode in the CA1 pyramidal layer at 0 s; 128 repetitions. Reversal occurred just below the pyramidal layer of CA1. Calibrations: c — 1 mV, 0.2 s; d — 1 mV. Positivity up.

er. In between the SPW-concurrent bursts virtually no activity occurred (Fig. 13). The number of complex-spike cells contributing to the burst varied between SPWs and most frequently it was impossible to tell the exact number of the participating neurons. Fig. 13d and e shows details of such synchronous complex-spike bursts. Isolated complex-spike cells fired with highest probability also during the SPWs, although some discharges could occur between them. It is important to emphasize that multiple complex-spike bursts never occurred during behaviors acompanied by RSA.

Interneurons in the CA1 region also fired synchronously with SPWs. Although they also discharged between the SPWs with single action potentials, during a SPW a burst of 10–25 action potentials could occur, with frequencies of up to 800 Hz (Fig. 13i). Although such a high rate of firing was frequently observed in response to electrical stimulation (Fig. 1), we have never seen it spontaneously except in association with SPWs. Interneurons in strata oriens, pyramidale and radiatum fired synchronously (Fig. 13f–h).

Granule cells also showed bursts of action potentials occasionally but SPWs were not recorded simultaneously from the microelectrode and the burst did not correlate with the SPWs derived from the CA1 region.

A depth profile of SPWs is illustrated in Fig. 14. In constructing depth profiles the amplitude of at least

both SPWs and theta waves derived from the microelectrode. h: interneuron in stratum radiatum of CA1 and locally recorded SPWs. i: detail of a burst with fast sweep. Same cell as in h. Note frequency increase up to 800 Hz. Calibrations: 20 μV (unit), 1 mV (EEG), 1 s (a), 0.2 s (b, c, f, g, h), 10 ms (d, e, i). Note opposite polarity in the polygraph record (a) and in b to i.

30 SPWs was measured at each recording depth and the profiles were compared with the simultaneously recorded field potentials evoked by either the commissural or the associational (Schaffer collaterals) input activation[25]. In 5 rats the last penetration was made with a 62 μm steel electrode. The phase reversal (n = 2) and the maximum negativity (n = 3) zones were marked with the Prussian blue reaction. The profiles of the SPWs and the field potential evoked by stimulation of Schaffer collaterals essentially coincided. In both cases the reversal occurred just below the pyramidal cell layer while the maximum negativity was seen in the middle portion of stratum radiatum. Consequently, the depth profile of the SPWs was different from that of RSA[30,53,141] (Figs. 14 and 7). In order to quantify the relationship between the burst of multiple cell discharges and SPWs, we cross-correlated the two events by triggering the analog averager with the multiple-unit bursts (Fig. 14d). Since the above results indicated that the multiple-spike burst in the CA1 region was mediated by way of the Schaffer collaterals, penetrations were made through the CA3b region in 6 rats. The amplitude of SPWs showed a progressively decreasing amplitude as the electrode penetrated the CA3 pyramidal layers and phase-reversal was observed in no case. However, despite the absence of the SPWs in the EEG, the bursting pattern of cell discharges was present in the CA3 region (Fig. 15a). Simultaneous recordings from the CA1 and CA3b pyramidal layer revealed that the multiple-spike bursts occurred virtually simultaneously in the two regions (Fig. 15b). Spike-triggered averaging with either the CA1 or CA3 bursts resulted in high amplitude SPW averages in CA1 but not in CA3 (Fig. 15c).

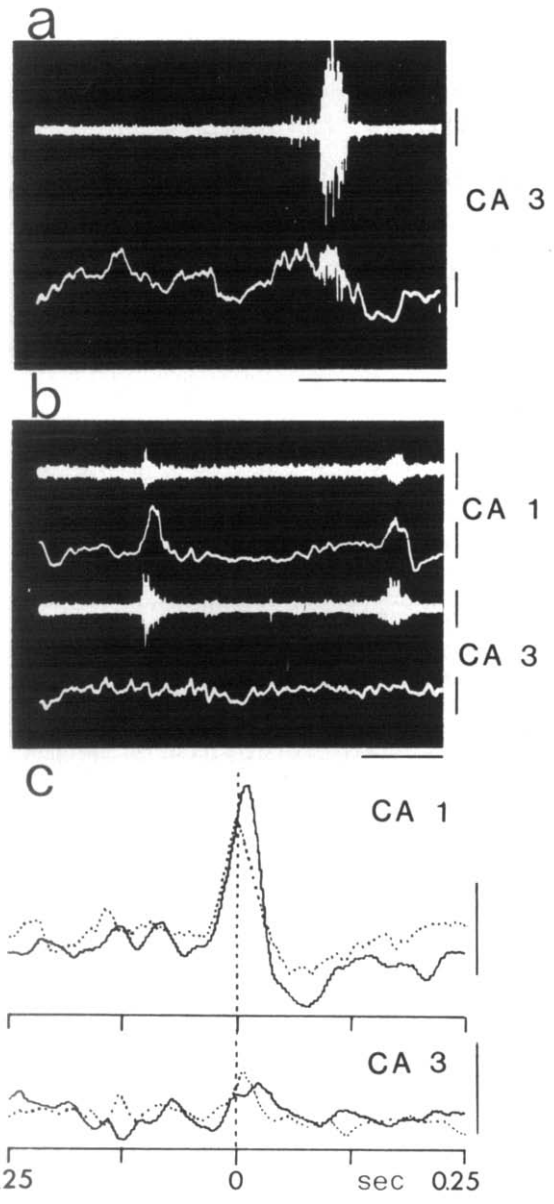

Fig. 15. a: multiple complex-spike burst and concurrently recorded local EEG in the CA3 pyramidal layer. b: EEG and multiple-unit activity recorded simultaneously from the pyramidal layers of CA1 (upper two traces) and CA3 (lower two traces) regions. c: spike-triggered averages of EEG recorded from the CA1 and CA3 pyramidal layers (1–30 Hz). The averager was triggered by the multiple complex-spike bursts of either CA1 (solid line) or CA3 (discontinuous line) at 0 s; 128 repetitions. Note the synchronous multiple unit bursts in CA1 and CA3 (b) and the absence of SPWs in CA3 (a–c). Calibrations: a, b — 10 μV (unit), 1 mV (EEG); c — 0.75 mV. Positivity up.

Fig. 16 summarizes the various manipulations attempting to dissociate the strict covariance of SPWs with behavior. Unilateral hippocampal lesions (n = 3) did not change this correlation. Atropine (50 mg/kg, i.p.), given to an intact rat was, in general, also ineffective. However, during small movements of the head and forelimbs, normally accompanied by RSA, SPWs were present in the hippocampal record. Although medial septum lesions abolished RSA (see above) movement still suppressed SPWs in these animals. However, section of the fimbria–fornix and the overlying neocortex abolished the correlation between behavior and the occurrence of SPWs. In these preparations, SPWs appeared in abundance without any regard to behavior. Isolation of the entorhinal cortex[136] did not change

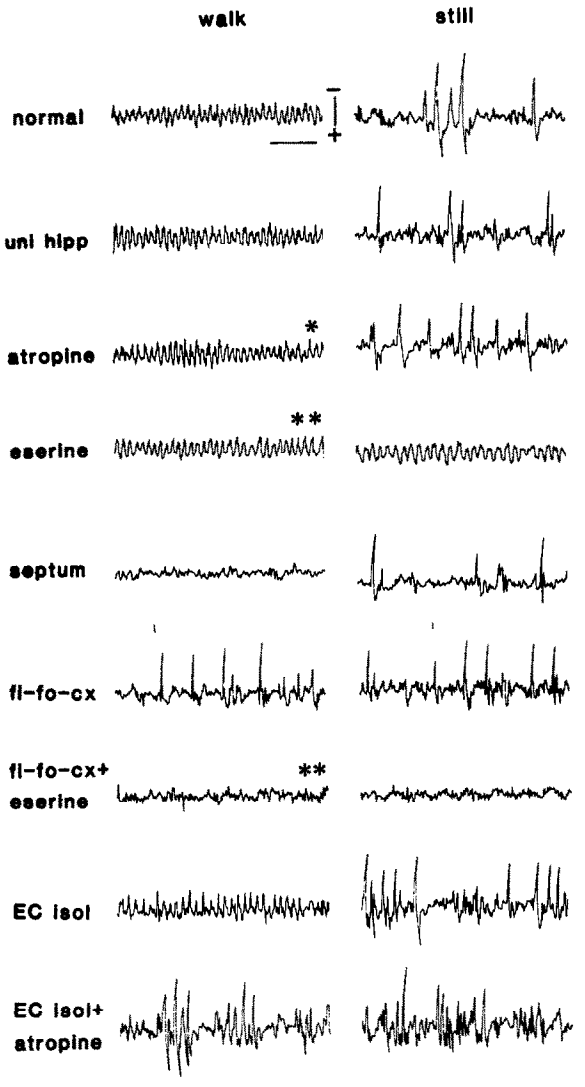

Fig. 16. Segments of polygraph records from stratum radiatum of CA1 during walking (walk) and immobility (still) following various manipulations. uni hipp, complete lesion of the contralateral hippocampus; atropine (50 mg/kg) and eserine (1 mg/kg) were administered intraperitoneally; septum, medial septum lesion. fi–fo–cx, surgical sectioning of the fimbria–fornix complex and the overlying neocortex. EC isol, isolation of the entorhinal cortex from its neocortical inputs; *SPWs were present during small head movements. **Crawling rather than walking. Calibrations: 1 mV, 1 s.

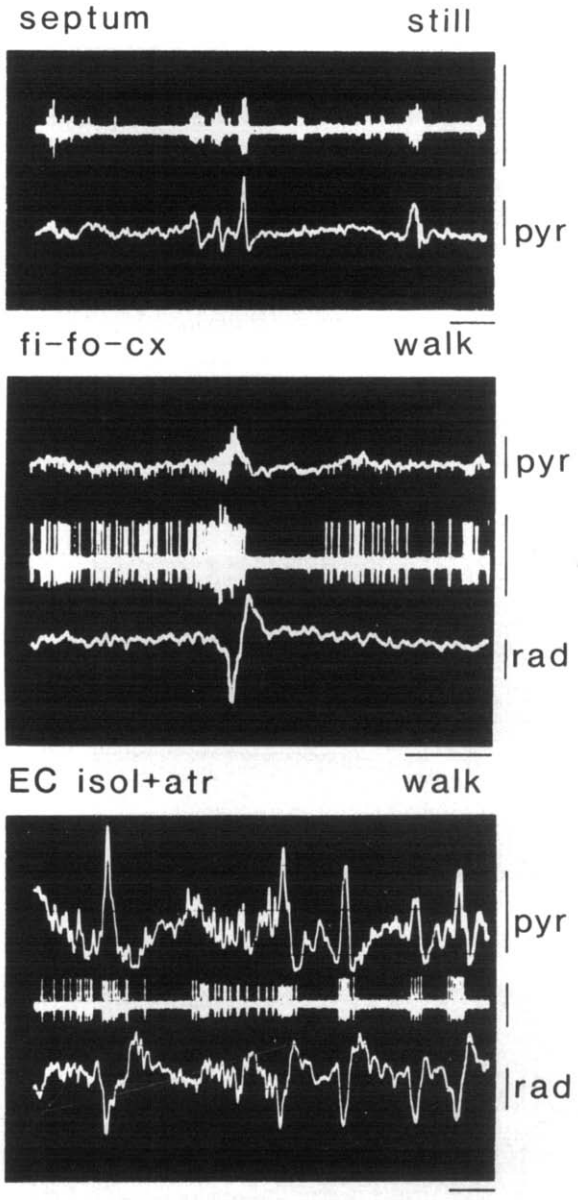

Fig. 17. Relationship between SPWs and unit activity following medial septum lesion (septum), sectioning of the fimbria–fornix complex and the overlying neocortex (fi–fo–cx), and after atropine administration to a rat with isolated entorhinal cortex (EC isol + atr). Upper panel: multiple complex-spike bursts in CA1 pyramidal layer during immobility (still). Middle and lower panels: interneuronal bursts in CA1 pyramidal layer with concurrent SPWs in strata pyramidale (pyr) and radiatum (rad) during walking. Calibrations: 100 μV (unit), 1 mV (EEG), 0.2 s. Positivity up.

the conditions under which SPWs occurred. However, if atropine was given to these rats, RSA during walking was abolished (see above) and was replaced by SPWs. Eserine (0.8–1 mg/kg, i.p.) was capable of completely suppressing SPW both in normal *and* in fi–fo–cx rats under all conditions. Following these various treatments SPWs were associated with the same cellular events as in the normal animal (Fig. 17).

CA3 pyramidal cells could be synchronously activated by means of electrical stimulation of the perfo-

rant path input to the dentate gyrus. This activation gave rise, in turn, to a volley in the Schaffer collaterals which produced a negative field potential in the stratum radiatum (sink) and a positive potential in the cell layer (source) of CA1. Such trisynaptic activation of CA1 pyramidal cell has been described in the anesthetized rabbit[6,11] and the drug-free rat during slow-wave sleep[142]. We frequently noticed the striking covariance of this field potential with ongoing behavior. Namely, the trisynaptic field response was virtually absent when the animal was walking, but present during behaviors like drinking, immobility and grooming (Fig. 18). The variability of the potential was quite large. Sometimes the potential was similar to the response obtained in the walking animal, other times it was of high amplitude (5–6 mV) occasionally followed by a second field potential of identical polarity. The latency between the onset of the first and second CA1 potentials was about 20 ms. Closer examination of the ongoing EEG record revealed that the amplitude variation of the CA1 potential was invariably related to the changes in EEG: stimulus volleys delivered during bursts of SPWs resulted in high-amplitude response, while small amplitude or no responses were evoked in their absence.

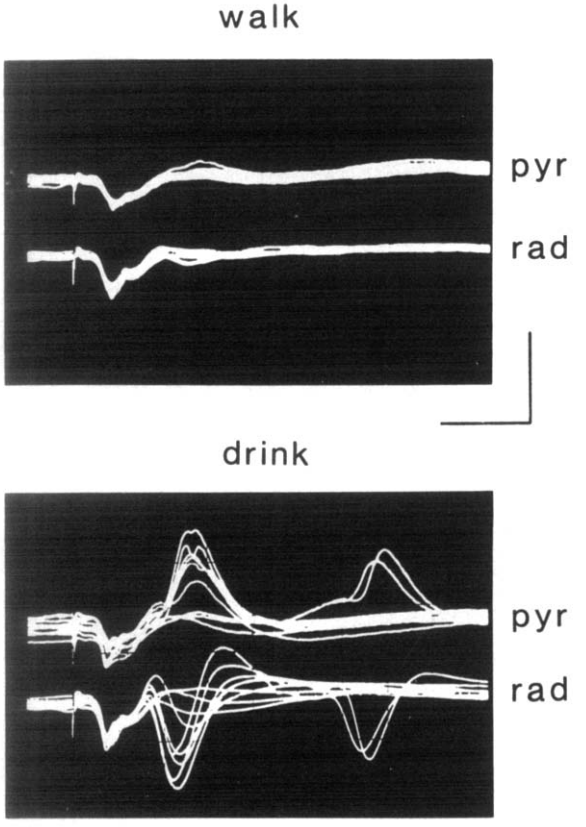

Fig. 18. Influence of behavior on the effectiveness of neuronal transmission through the hippocampal formation. Stimulation was applied to the angular bundle, and responses were recorded in strata pyramidale (pyr) and radiatum (rad) of CA1. The phase-reversed potentials represent multisynaptic excitation of the apical dendrites of CA1 pyramidal cells through the Schaffer collaterals[6,11,142]. The early response is a volume conducted potential from the dentate gyrus (note absence of phase-reversal). Ten superimposed sweeps each. Note lack of the CA1 response during walking. Microelectrode in stratum radiatum was 0.8 mm posterior to reference electrode in the pyramidal layer. Calibrations: 5 mV, 10 ms. Positivity up.

3.4. *Hippocampal fast activity (25–70 Hz)*

Fast activity occurred under all behavioral conditions. It was usually superimposed on slow waves but occasionally it appeared in isolation between SPWs. In agreement with previous investigations on anesthetized animals[18,21,125] the amplitude depth-profile of the power of fast activity (25–70 Hz) showed two peaks: a narrow peak at the level of the pyramidal layer of CA1 and a larger and broader peak in the granule cell layer and the hilus. The phase spectra indicated a consistent sharp phase-reversal just below the pyramidal cell layer (Fig. 7a). In some, but not all animals, a second phase-reversal occurred across the granule cell layer, but we failed to find the source of this inconsistency. If electrodes were positioned bilaterally and symmetrically in the hili, high coherence values were obtained in the 25–70 Hz band and the phase spectra indicated that the signals were completely 'in-phase'. The power of fast activity was higher during walking and running as compared with the power obtained during immobility and drinking (Fig. 19a). Occasionally this difference was also observable in the 30–70 Hz band of the unit power histogram (e.g. Fig. 4). Spike-triggered averaging revealed a consistent relationship between fast EEG activity and unitary discharges. Averages of the highest amplitude were obtained from the hilus, followed by the pyramidal cell layer of CA1. Comparison of averages obtained by using different cell types of the same region in the same animal showed that the correlation between unit firing and the fast EEG pattern was highest with interneurons and granule cells. Averages triggered by complex-spike cells revealed little periodicity in the fast EEG band. With inter-

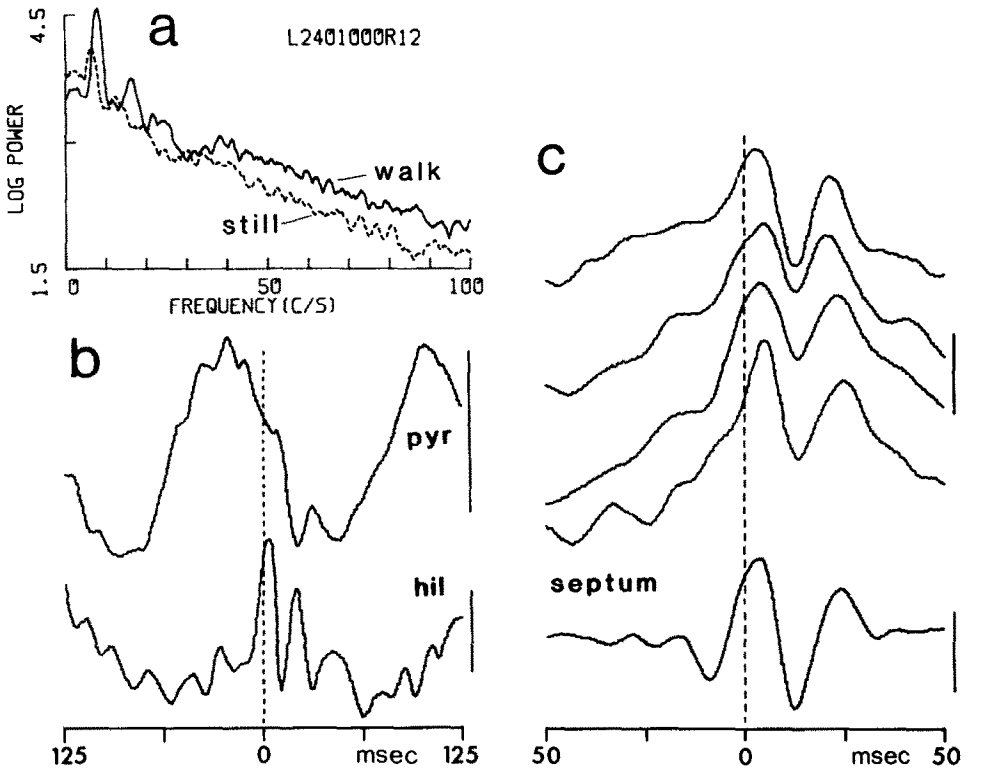

Fig. 19. Logarithmic power spectra of EEG from the hilus during walking and immobility (still). Note higher power of fast activity (25–100 Hz) during walking. b: spike-triggered averages of EEG from CA1 pyramidal layer (pyr) and the hilus (hil) during walking (1–100 Hz); 512 repetitions. c: EEG averages (1–100 Hz) recorded from the hilus in 4 different intact animals and in a rat with septal lesion (septum), 1024 repetitions. Note superimposition of the high frequency periodicity (30–50 Hz) on RSA waves. The averager was triggered by hilar interneurons in all cases. Calibration: 100 μV.

neurons, consistent averages were obtained by averaging 512 EEG segments. The periodicity of the first few waves varied between 35 and 60 Hz (Fig. 19). This high frequency periodicity was superimposed on slow waves. Fast activity was dominant around the positive peak of RSA waves both in the hilus (Fig. 19) and in CA1 (Fig. 20). The relationship between cell firing and fast EEG waves remained after medial septum lesions (Fig. 19, septum). Amplitude depth-profiles of the fast activity in septal animals were identical with those obtained in normal rats. Following urethane anesthesia EEG power in the 25–50 Hz band increased while higher frequency components (50–100 Hz) considerably decreased as compared to walking in the waking rat. Coherence between unit activity and EEG (25–50 Hz) as well as between pairs of EEG traces recorded from different cytoarchitectonic regions also increased (Fig. 20).

4. DISCUSSION

4.1. *Feed-forward inhibition from the septum*

In a now classic paper Fujita and Sato[48] reported that the membrane potential of pyramidal cells showed synchronous fluctuations with the hippocampal RSA. Furthermore, the positive- and negative-ongoing phases of the EEG recorded just outside the cell corresponded to the hyperpolarization and depolarization phases of the intracellular (presumably pyramidal cell) recording, respectively. This finding, and others, demonstrate that the grouped excitatory cholinergic input[88,92,123] from the pacemaker cells of the septum[12,54,85,102] impinges upon the pyramidal cells during RSA, resulting in rhythmic EPSPs and occasionally action potentials. Discharges of the pyramidal cells may excite inhibitory interneurons which

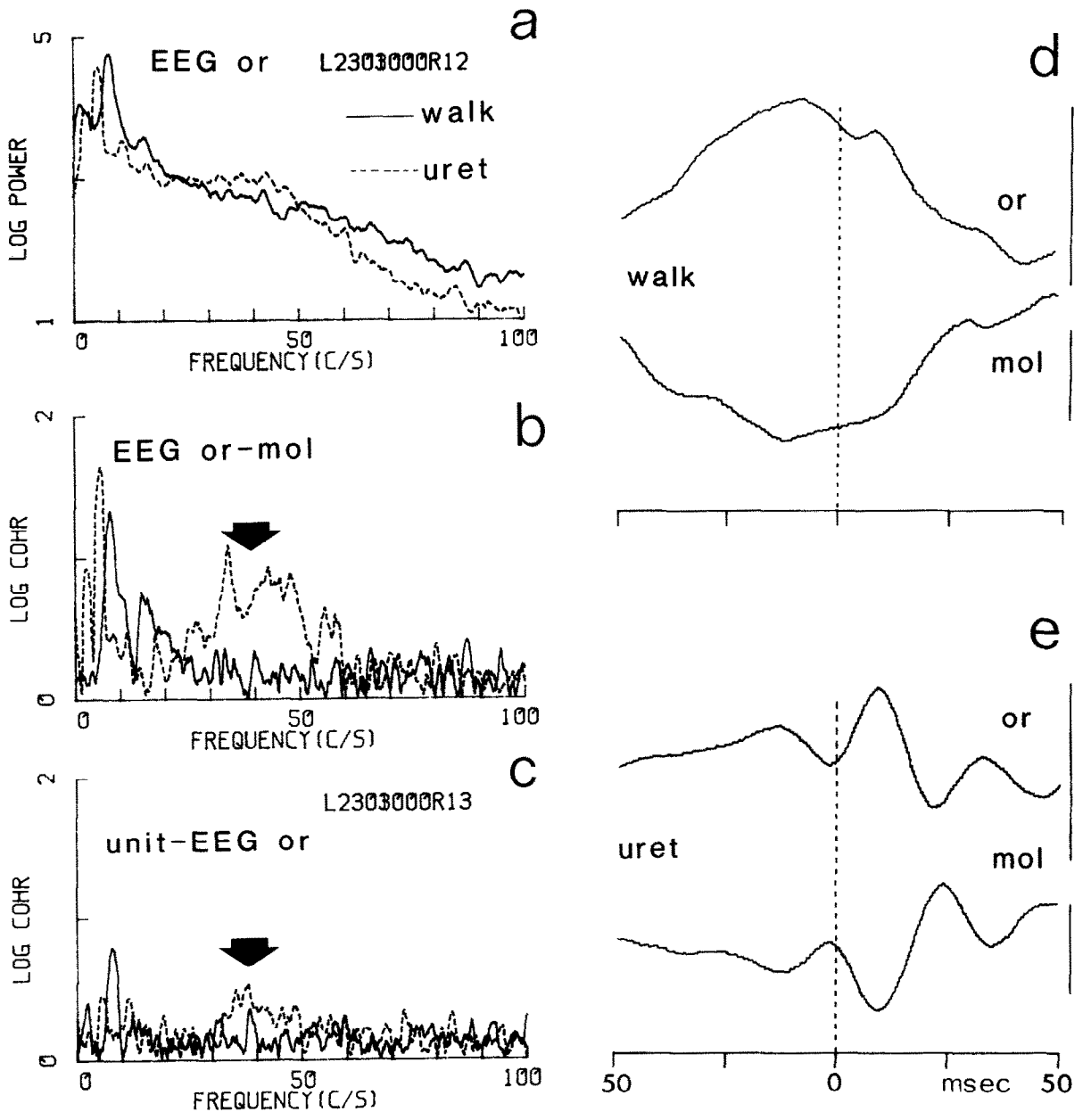

Fig. 20. Influence of urethane on fast activity. a: logarithmic power spectra of EEG recorded from stratum oriens of CA1 (or) during walking and urethane anesthesia. Note decrease of power in the 50–100 Hz band and increase in 25–50 Hz. b: z-transform coherence spectra between pairs of EEG derived from fixed electrodes in stratum oriens of CA1 and molecular layer of the dentate gyrus (mol) before and after urethane. Note increase of coherence in the 25–50 Hz band after urethane (black arrow). c: z-transform coherence-spectra between interneuronal activity in CA1 pyramidal layer and EEG. Note increase of coherence (25–50 Hz) after urethane. d, e: spike-triggered averages of EEG during walking and urethane anesthesia (1–100 Hz). The averager was triggered by an interneuron in CA1 pyramidal layer at 0 s. 1024 repetitions. Note increase of rhythmicity after urethane (e). Calibration: 100 μV. Positivity up.

in turn generate IPSPs in the soma[8,13,39,58,59].

In agreement with this model we found that in the freely moving rat pyramidal cells (complex-spike cells) in the CA1 region fired significantly more frequently on the negative phase of the locally derived RSA than on the positive phase[19,48,143,144]. Interneurons in this region showed an opposite relationship. Several lines of evidence suggest, however, that

these interneurons were not exclusively excited by the recurrent circuit: (1) With the appearance of hippocampal RSA the firing frequency of the pyramidal cells decreased while that of the interneurons increased. The general decrease in the firing rate of pyramidal cells during RSA is in line with several earlier observations. In acute studies, activation of the septo-hippocampal pathways by means of electrical stimulation of various subcortical areas, by stimulation of a peripheral nerve or by sensory stimulation decreased the probability of discharge of pyramidal cells[13,39,42,55,58,59,65,86]. Furthermore, arousing stimuli evoking hippocampal RSA had a suppressive effect on complex-spike cells in awake rabbits[79] and rats[34,89]. The paradoxical phase of sleep which is accompanied by high amplitude RSA and, in general, by the lowest level of discharge frequency of complex-spike cells[15,94,96,101,105]. Physiologically identified or putative interneurons ('theta' cells[105]) on the other hand, invariably increase their firing rate during RSA[13,34,44,45,105,119]. If interneurons are driven exclusively disynaptically through the recurrent collaterals of pyramidal cells it is difficult to understand this inverse relationship. (2) Interneurons in the stratum radiatum of CA1 shared functional characteristics with the interneurons of stratum oriens and pyramidale including phase-relation with RSA. These neurons are probably not innervated by the pyramidal cells since no axon collaterals were observed in the radiatum[41,69]. (3) On the basis of the short axon collaterals and the low threshold of interneurons[26] one might expect a short time delay between the discharges of pyramidal cells and interneurons. Indeed, when interneurons of strata oriens and radiatum of CA1 are driven recurrently (e.g. during sharp waves) they fire virtually in synchrony with the pyramidal cells. (4) Section of the fimbria–fornix and atropine treatment both increased the firing rate of complex-spike cells and the incidence of sharp waves. Eserine, on the other hand, completely suppressed the occurrence of sharp waves and the concurrent multiple burst discharges of the complex-spike cells.

We propose an alternative circuitry which offers a parsimonious explanation of the above findings. We suggest that in addition to excitation via the recurrent path, interneurons of all 3 layers of the CA1 region are directly excited by the septal pacemaker cells. Such a feed-forward mechanism would account for the inverse relations of pyramidal cells and interneurons with respect to firing rate and phase of RSA. Discharges of the rhythmically inhibited pyramidal cells would occur when excitatory inputs are also activated but at a small probability at times when inhibitory interneurons fire maximally. The proposed circuitry is supported by anatomical and histochemical data. The distribution of septal projections and acetylcholinesterase (AChE) activity coincides well with the distribution of the interneurons in the stratum oriens, radiatum and the hilus of the dentate gyrus[71,84,88,92,123,138]. It is worth emphasizing that the reaction product is intercellular and the pyramidal cells and granule cells are devoid of AChE activity in their cytoplasm[88,138]. On the other hand, local circuit neurons in the stratum oriens and radiatum of the Ammon's horn and the polymorphic zone of the hilus display strong AChE activity[88,138]. Finally, there is no anatomical evidence that the septal cholinergic input synapses with the pyramidal cells or granule cells but the data do suggest that the septal projection terminates on the interneurons[84,97,112].

Interneurons and granule cells of the dentate gyrus did not show the inverse correlation observed in the CA1 region. This question will be elaborated below.

4.2. *Is the septal input sufficient for RSA?*

Atropine did not abolish all RSA in the freely moving rat. Although small movements of the head and limbs were no longer accompanied by RSA, during walking and running it was clearly present. Rhythmicity of interneurons and the coherence between unit firing and RSA decreased considerably after atropine, but was not completely lost. A non-cholinergic RSA input may be inferred but this apparently does not come from the septum but from the entorhinal cortex. In rats with entorhinal cortex isolation or entorhinal cortex lesions[135,136] atropine completely abolished hippocampal RSA.

Reciprocal firing rates and opposite phase relations to RSA of principal cells as compared to interneurons were not observed in the dentate gyrus. Granule cells, complex-spike cells and the majority of interneurons fired preferentially on the positive phase of the locally derived RSA. The following considerations make it unlikely, however, that this finding reflects only a cholinergic septal input driving the

principal cells and, thereby, the recurrent inhibitory circuitry. First, Bland et al.[20] reported that atropine did not specifically antagonize the action of locally applied acetylcholine on dentate granule cells. Second, there is a lack of evidence for a direct cholinergic projection from septal cells to granule cells[84]. Third, in a recent computer simulation model proximal excitation of the somatic segments of the granule cells (region where septal synapses may occur) was found to be an unlikely mechanism to account for the empirical RSA phase profile. Instead, the best approximation was achieved with models requiring distal dendritic excitation of both granule cells and pyramidal cells[61]. Finally, in urethane anesthetized rats, granule cells and interneurons were found to discharge mainly on opposite phases of the theta cycle[144].

A second possible source of rhythmical input to the hippocampus is the entorhinal cortex[35,135]. RSA recorded in layer III of the entorhinal cortex was similar in phase and wave shape to RSA recorded in the pyramidal cell layer of CA1, and RSA in layers II–I was similar to that recorded in the molecular layer of the dentate gyrus[95]. RSA signals of layers III and II yielded phase-shifts of 50–160°. It is relevant to mention that the pyramidal cells of layer III and stellate cells of layer II are the anatomical origin of the afferent inputs to the CA1 and dentate regions, respectively[122]. Rhythmical discharge of these neurons at RSA frequency would provide an excitatory input to the dendrites of both pyramidal and granule cells. The possible pathways for the mediation of 'pacemaker' activity from the septum to the entorhinal cortex will be discussed elsewhere[136].

4.3. *Sharp waves and the intrahippocampal circuitry*

Sharp waves were recorded from the CA1 region[100,126]. Depth profile experiments revealed that their origin is the active depolarization (sink) of the apical dendrites via the Schaffer collaterals. The strong synaptic drive during SPWs led to the synchronous discharge of many CA1 pyramidal cells[126]. Concurrent bursting of interneurons could be brought about by converging excitation of the recurrent collaterals of the CA1 pyramidal cells or by direct excitation by the Schaffer collaterals[26]. Simultaneous recordings from the CA3 and CA1 regions disclosed that the CA3 region might act as a trigger zone for the synchronized discharge. A possible mechanism of such triggering action is the mutual excitation of neighboring pyramidal cells. Since excitatory interneurons are not known in the hippocampus, pyramidal cells are assumed to excite one another directly by their recurrent axon collaterals[41,69,75] or by electronic junctions[87].

SPWs were never observed during behaviors accompanied by RSA. We suggest that two separate systems might be responsible for the suppression of SPWs (Fig. 16) during RSA. The first one is a cholinergic septo-hippocampal path. Activation of this system alone is sufficient to suppress multiple bursting of pyramidal cells. In support of this, eserine was found to suppress SPWs under all conditions, probably by its cholinomimetic action on the inhibitory interneurons. The second suppressive system is probably multisynaptic. Its origin is not known but it courses presumably in the cingulate cortex and neocortex[136]. This system might be responsibe for the movement-concurrent suppression of SPWs following atropine or a septal lesion. Elimination of both suppressive systems (e.g. by entorhinal cortex isolation and atropine together of fi–fo–cx lesion) resulted in behavior-independent occurrence or SPWs. Additional support for the behavior-dependent operation of the intrahippocampal circuitry comes from the evoked potential experiment. During RSA-related behaviors stimulation of the perforant path failed to induce a Schaffer collateral response in the CA1 region, while large amplitude, sometimes double responses were present during drinking and immobility. Taken together these findings indicate that in the absence of RSA a synchronous volley initiated in the entorhinal cortex activates synapses successively in dentate gyrus, CA3, and CA1[6,50,73,113,130]. The CA1 region in turn might project this afferent copy[62] back to the retrohippocampal structures including the entorhinal cortex. During RSA related behaviors this intrahippocampal circuitry is blocked at some level.

Finally, it is relevant to note that the described physiological features which characterize the cellular basis of SPWs (intrinsic bursting property, mutual excitation, and disinhibition) are frequently applied in experimental models of epilepsy[103,131].

4.4. *Fast activity*

A number of different observations are consistent with the hypothesis that hippocampal fast activity (25–70 Hz) results from the synaptic action of interneurons on the soma region of principal cells. (1) Amplitude depth profiles revealed peaks in the pyramidal cell layer of CA1 and the granule cell layer/hilar region[21]. The highest amplitude spike-triggered averages (25–70 Hz) were obtained also from these layers. (2) Phase-reversals were observed just below the pyramidal layer and sometimes below the granule cell layer. (3) The periodicity of spike-triggered averages (25–70 Hz) corresponded to the frequency peaks of EEG and unit activity obtained with the spectral method. (4) Increase of the firing rate of interneurons concurrent with the appearance of RSA was accompanied by an increase of the EEG and unit power in the 25–70 Hz band. (5) Following urethane anesthesia the increase of the interspike intervals of interneurons was accompanied by a downward shift of the frequency peak in the EEG power spectrum (25–70 Hz). (6) Fast activity persisted following various deafferentations of the hippocampus. (7) The phase-relationship of RSA and fast waves was similar to the maximum probability of firing of interneurons in relation to RSA waves. (8) Fast waves could be simulated by the intrinsic circuitry within the hippocampus[77].

4.5. *Model of RSA generation*

The model (Fig. 21) assumes the existence of 4 separate inputs representing the perforant path which excites (1) the dendrites of CA1 pyramidal cells and (2) the dendrites of granule cells, and the septal inputs which excite (3) CA1 interneurons, and (4) dentate interneurons. The interneurons are then assumed to inhibit the pyramidal and granule cells at their somata. Somatic inhibition and dendritic excitation arrive nearly synchronously (i.e. in the same phase of a theta wave), but inputs to CA1 and the dentate gyrus are phase-shifted, and are suggested to derive from different 'pacemaker' cells in the septum[30].

Pyramidal and granule cells are assumed to generate the currents and potential field of RSA within the hippocampus. Membrane potential changes of interneurons are not presumed to contribute to the field RSA significantly, because of the small proportion of these cells, their geometry and scattered locations[106]. It is assumed that each of the 4 rhythmic inputs can generate a dipole RSA field on its own. Dendritic excitation by perforant path results in an active sink in the dendrites, accompanied by passive sources from the cell bodies, giving rise to dendritic negativity and soma-positivity[61]. Somatic inhibition by interneurons generates somatic hyperpolarization (active sources) accompanied by dendritic passive sinks[76]. On account of volume conduction[46,61,82], the 4 separate RSA dipole generators will contribute to the amplitude and phase profile of the RSA with depth. The actual amplitude and phase profile will depend on the relative strength and depth profile of each dipole generator[27,28,106]. The probability of cell discharge and consequently the relationship between cell firing and the phase of field RSA will be a function of the relative strength of somatic inhibition and distal dendritic excitation. Pyramidal cells in CA1 were found to fire at a very low rate and on the negative phase of the pyramidal layer RSA. Granule cells, on the other hand, considerably increased their frequency during movement-concurrent RSA[111] and fired preferential-

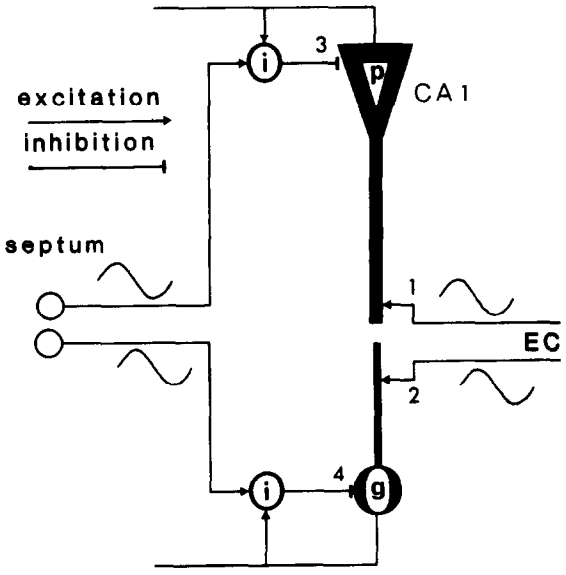

Fig. 21. Model of hippocampal RSA. The model assumes four independent rhythmic inputs (1–4), each of which is capable of generating field RSA. Inputs to the same neurons are nearly synchronous (1–3 and 2–4), but inputs to the pyramidal cells (p) and granule cells (g) are phase-shifted. i, inhibitory interneuron.

ly on the positive portion of the locally derived RSA waves. We could account for the opposite phase-relationships by assuming that the perforant path input to CA1 pyramidal cells is considerably less effective than the perforant path input to the granule cells. Andersen et al.[2,10,11] found that stimulation of the entorhinal area could initiate a field potential in CA1 but failed to evoke action potentials of the pyramidal cells. On the other hand, perforant path activation is very effective in evoking synchronous discharges of the granule cells[2,5,10,11,23,80]. Recent anatomical findings indicate that at least some interneurons in CA1 terminate exclusively on the axon initial segment of pyramidal cells[98], which may serve as a powerful inhibitory mechanism. On the other hand basket neurons in the dentate gyrus form exclusively symmetric synapses with the somata, proximal dendrites and dendritic spines of granule cells[109]. An additional mechanism may be inferred from the observation of Andersen et al.[7] that iontophoretically applied GABA to the distal dendritic region of the pyramidal cells resulted in *depolarization* and increased membrane conductance, suggesting that GABAergic inhibitory interneurons at the distal region of the stratum radiatum would slowly depolarize the membrane and shunt the currents from neighboring excitatory synapses. Our finding that interneurons in the stratum radiatum fired in synchrony with interneurons of strata oriens and pyramidale suggests that this 'discriminative' depolarizing inhibitory mechanism[7] may further reduce the excitatory effect of the entorhinal input to CA1.

According to the model any one input alone is sufficient for RSA generation in the hippocampus. Despite some obvious changes, RSA is present after blocking the cholinergic septo-hippocampal input by atropine[70,134]. Also, atropine-sensitive RSA in the urethane anesthetized rabbit remained unchanged following complete removal of the subicular complex together with the overlying alveus and angular bundle[4]. The present experiment found that, following urethane anesthesia, interneurons retained their phase-relationship with slow waves. This is different from the relation of pyramidal cells during SPWs when both types of cells fired in synchrony on the local positive wave.

No consideration has been given to the role of the CA3 region in the present model. It has been claimed that RSA is not generated in this region[18,27,29]. That CA3–CA1 interactions play no role or a negligible role in the generation of CA1 RSA is supported by our finding that the trisynaptic path is blocked in the presence of RSA, as well as by a recent report that, following kainic acid lesion of CA3 pyramidal cells, hippocampal RSA remained unchanged[140].

While solid evidence in support of some parts of this model is insufficient, the present model explains considerably more empirical data than previous ones. Specific predictions can be tested experimentally.

5. SUMMARY

Rats implanted with recording and stimulating electrodes were trained to run in an activity wheel for a water reward. Unitary discharges and slow activity were recorded by a movable tungsten microelectrode and by fixed electrodes. Single cells were classified according to their spontaneous and evoked response properties as pyramidal cells, granule cells and interneurons. Unit activity, EEG and their interrelations were studied by spectral and spike-triggered averaging methods. Gradual phase-shifts of RSA were observed both in CA1 and the dentate gyrus. Movement-related RSA was correlated with a decrease in firing rate of pyramidal cells and an increase in the firing of both interneurons and granule cells. In the CA1 region pyramidal cells and interneurons fired preferentially on the negative and positive phases of the locally derived RSA, respectively. In the dentate gyrus both granule cells and interneurons discharged mainly on the positive portion of the local RSA waves, about 90° before the CA1 pyramidal cells. Fourier analysis of the spike trains of interneurons and granule cells showed high power at RSA frequency, coherent with the concurrent EEG. Phase relations between discharges of interneurons and RSA remained unchanged following urethane anesthesia. In waking rats, atropine administration resulted in a decreased discharge of interneurons at RSA frequency, and reduced coherence with RSA. Lesions of the septum or the fimbria–fornix abolished RSA and the rhythmic discharges of the interneurons. Isolation of the entorhinal cortex (EC) from its cortical inputs did not change either EEG or neuronal firing. However, in such a preparation atropine

completely abolished RSA and related rhythmicity of interneurons. During drinking and immobility but not during walking, sharp waves (SPW) of about 40–100 ms duration appeared in the EEG. SPWs were invariably accompanied by synchronous discharges of several pyramidal cells and interneurons. CA3 pyramidal cells also discharged in synchronous bursts but without local SPWs. Laminar profiles of SPWs and the field potentials evoked by stimulation of Schaffer collaterals were essentially identical. The behavior-dependent occurrence of SPWs was retained following atropine administration, septal lesion or EC isolation but was lost after fimbria–fornix–neocortex lesion or following atropine administration in EC isolated rats. In addition to relations to RSA and SPWs, interneurons were phase-locked to the fast EEG pattern (25–70 Hz). This relationship was preserved following lesions of the septum or the fimbria–fornix complex. The above findings allowed us to construct a new model of hippocampal RSA generation based on feed-forward inhibition from the septum and a direct excitation by the entorhinal input. SPWs are suggested to reflect strong synaptic activation of CA1 pyramidal cells via the Schaffer collaterals as a consequence of synchronous discharges of CA3 pyramidal neurons. Fast activity is supposed to reflect synaptic activity close to the somata of pyramidal cells and granule cells.

ACKNOWLEDGEMENTS

We thank R. K. Cooley, D. Steward and D. Batliwalla for technical help and Lynne Mitchell for typing the manuscript. Supported by NSERC Grants A0118 and U0052.

REFERENCES

1 Amaral, D. G., A Golgi study of cell types in the hilar region of the hippocampus of the rat, *J. comp. Neurol.*, 182 (1978) 851–914.
2 Andersen, P., Organization of hippocampal neurons and their interconnections. In R. L. Isaacson and K. H. Pribram (Eds.), *The Hippocampus, Vol. 1.* Plenum, New York, 1975, pp. 155–175.
3 Andersen, P. and Anderson, S. A., *Physiological Basis of the Alpha Rhythm,* Appleton, New York, 1968.
4 Andersen, P., Bland, B. M., Myhrer, T. and Schwartzkroin, P. A., Septo-hippocampal pathway necessary for dentate theta production, *Brain Research,* 165 (1979) 13–22.
5 Andersen, P., Bliss, T. V. P. and Skrede, K. K., Unit analysis of hippocampal population spikes, *Exp. Brain Res.*, 13 (1971) 208–221.
6 Andersen, P., Bliss, T. V. P. and Skrede, K. K., Lamellar organization of hippocampal excitatory pathways, *Exp. Brain Res.*, 13 (1971) 222–238.
7 Andersen, P., Dingledine, R., Gjerstad, L., Lanøgmoen, I. A. and Laursen, A. M., Two different responses of hippocampal pyramidal cells to application of gamma-amino butyric acid, *J. Physiol. (Lond.),* 305 (1980) 279–296.
8 Andersen, P. and Eccles, J. C., Inhibitory phasing of neuronal discharge, *Nature (Lond.),* 196 (1962) 645–647.
9 Andersen, P., Eccles, J. C. and Løyning, Y., Pathways of postsynaptic inhibition in the hippocampus, *J. Neurophysiol.*, 27 (1964) 608–619.
10 Andersen, P., Holmquist, B. and Voorhoeve, P. E., Entorhinal activation of dentate granule cells, *Acta physiol. scand.*, 66 (1966) 448–460.
11 Andersen, P. and Løyning, Y., Interaction of various afferents on CA1 neurons and dentate granule cells. In P. Passouant (Ed.), *Physiologie de l'Hippocampe,* CNRS, Paris, 1962, pp. 23–45.
12 Apostol, G. and Creutzfeldt, O. D., Cross correlation between the activity of septal units and hippocampal EEG during arousal, *Brain Research,* 67 (1974) 65–75.
13 Artemenko, D. P., Role of hippocampal neurons in theta-wave generation, *Neirofiziologiya,* 4 (1972) 531–539 (in Russian).
14 Beckstead, R. M., Afferent connections of the entorhinal area in the rat as demonstrated by retrograde cell-labeling with horseradish peroxidase, *Brain Research,* 152 (1978) 249–264.
15 Belugou, F. L., Benoit, O. and Leygonie, F., Décharges neuronales de l'hippocampe au cours de la veille et du sommeil, *J. Physiol. (Paris),* Suppl. 2 (1968) 399.
16 Blackstad, T., Commissural connections of the hippocampal region in the rat, with special reference to their mode of termination, *J. comp. Neurol.*, 105 (1956) 417–538.
17 Blackstad, T. W. and Flood, P. R., Ultrastructure of hippocampal axosomatic synapses, *Nature (Lond.),* 198 (1963) 542–543.
18 Bland, B. H., Andersen, P. and Ganes, T., Two generators of hippocampal theta activity in rabbits, *Brain Research,* 94 (1975) 199–209.
19 Bland, B. H., Andersen, P., Ganes, T. and Sveen, O., Automated analysis of rhythmicity of physiologically identified hippocampal formation neurons, *Exp. Brain Res.*, 38 (1980) 205–219.
20 Bland, B. H., Kostopoulos, D. W. and Phillis, J. W., Acetylcholine sensitivity of hippocampal formation neurons, *Canad. J. Physiol. Pharmacol.*, 52 (1974) 966–971.
21 Bland, B. H. and Whishaw, I. Q., Generators and topography of hippocampal theta (RSA) in the anesthetized and freely moving rat, *Brain Research,* 118 (1976) 259–280.
22 Buzsáki, G., Bors, L., Nagy, F. and Eidelberg, E., Spatial mapping, working memory and the fimbria–fornix system, *J. comp. Physiol. Psychol.*, 96 (1982) 26–34.
23 Buzsáki, G. and Czeh, G., Commissural and perforant

path interactions in the rat hippocampus: field potentials and unitary activity, *Exp. Brain Res.*, 43 (1981) 429–438.
24 Buzsáki, G. and Eidelberg, E., Commissural projections to the dentate gyrus of the rat: evidence for feed-forward inhibition, *Brain Research*, 230 (1981) 346–350.
25 Buzsáki, G. and Eidelberg, E., Convergence of associational and commissural pathways on CA1 pyramidal cells of the rat hippocampus, *Brain Research*, 237 (1982) 283–295.
26 Buzsáki, G. and Eidelberg, E., Direct afferent excitation and long-term potentiation of hippocampal interneurons, *J. Neurophysiol.*, 48 (1982) 597–607.
27 Buzsáki, G., Grastyán, E., Haubenreiser, J., Czopf, J. and Kellényi, L., Hippocampal slow wave activity: sources of controversy. In C. Ajmone Marsan and H. Matthies (Eds.), *Neuronal Plasticity and Memory Formation*, Raven Press, New York, 1982, pp. 511–529.
28 Buzsaki, G., Grastyan, E., Kellenyi, L. and Czopf, J., Dynamic phase-shifts between theta generators in the rat hippocampus, *Acta. physiol. Acad. Sci. hung.*, 53 (1979) 41–45.
29 Buzsáki, G., Haubenreiser, J., Grastyan, E., Czopf, J. and Kellényi, L., Hippocampal slow wave activity during appetitive and aversive conditioning in the cat, *Electroenceph. clin. Neurophysiol.*, 51 (1981) 276–290.
30 Buzsáki, G., Leung, L. S. and Vanderwolf, C. H., Phase-profile of theta activity in the dentate gyrus of the freely moving rat, submitted.
31 Chronister, R. B. and DeFrance, F. F., Organization of projection neurons of the hippocampus, *Exp. Neurol.*, 66 (1979) 509–523.
32 Crutcher, K. A., Madison, R. and Davis, J. N., A study of the rat septo-hippocampal pathway using anterograde transport of horseradish peroxidase, *Neuroscience*, 16 (1981) 1961–1973.
33 Curtis, D. R., Felix, D. and McLellan, H., GABA and hippocampal inhibition, *Brit. J. Pharmacol.*, 40 (1970) 881–883.
34 Delacour, J., Conditioned modifications of arousal and unit activity in the rat hippocampus, *Exp. Brain Res.*, 38 (1980) 95–101.
35 Destrade, C. and Ott, T., Modulation of memory by hypothalamic post-trial stimulation driving two types of hippocampal rhythmical slow activity. In C. Ajmone Marsan and H. Matthies, (Eds.), *Neuronal Plasticity and Memory Formation*, Raven Press, New York, 1982, pp. 495–509.
36 Domesick, V. B., Projections from the cingulate cortex in the rat, *Brain Research*, 12 (1969) 269–320.
37 Eccles, J. C., *The Inhibitory Pathways of the Central Nervous System*, Thomas, Springfield, IL, 1969.
38 Elul, R., The genesis of EEG, *Int. Rev. Neurobiol.*, 15 (1972) 227–272.
39 von Euler, C. and Green, J. D., Excitation, inhibition and rhythmical activity in hippocampal pyramidal cells in rabbit, *Acta. physiol. scand.*, 48 (1960) 110–125.
40 Finch, D. M. and Babb, T. L., Response decrement in a hippocampal basket cell, *Brain Research*, 130 (1977) 354–359.
41 Finch, D. M. and Babb, T. L., Demonstration of caudally directed hippocampal efferents in the rat by intracellular injection of horseradish peroxidase, *Brain Research*, 214 (1981) 405–410.
42 Finch, D. M., Feld, R. E. and Babb, T. L., Effects of mesencephalic and pontine electrical stimulation on hippocampal neuronal activity in drug-free cat, *Exp. Neurol.*, 61 (1978) 318–336.
43 Fox, S. E. and Ranck, J. B. Jr., Localization and anatomical identification of theta and complex-spike cells in dorsal hippocampal formation of rats, *Exp. Neurol.*, 49 (1975) 299–313.
44 Fox, S. E. and Ranck, J. B. Jr., Electrophysiological characteristics of hippocampal complex-spike cells and theta cells, *Exp. Brain Res.*, 41 (1981) 399–410.
45 Fox, S. E., Wolfson, S. and Ranck, J. B. Jr., Investigating the mechanism of hippocampal theta rhythms: approaches and progress. In W. Seifert (Ed.), *Molecular Cellular and Behavioral Neurobiology of the Hippocampus*, Academic Press, New York, 1983.
46 Freeman, W. J., *Mass Action in the Nervous System*, Academic Press, New York, 1975.
47 Fricke, R. and Cowan, W. M., An autoradiographic study of the development of the entorhinal and commissural afferents to the dentate gyrus of the rat, *J. comp. Neurol.*, 173 (1977) 231–250.
48 Fujita, Y. and Sato, T., Intracellular records from hippocampal pyramidal cells in rabbits during theta rhythm activity, *J. Neurophysiol.*, 27 (1964) 1011–1025.
49 Fuxe, K., Hökfelt, T., Johansson, D., Jonsson, A., Lidbrink, P. and Ljungdahl, A., The origin of the dopamine nerve terminals in limbic and frontal cortex. Evidence for mesocortical dopamine neurons, *Brain Research*, 82 (1974) 349–355.
50 Gaarskjaer, F. B., Organization of the mossy fiber system of the rat studied in extended hippocampi: I. Terminal area related to the number of granule and pyramidal cells, *J. comp. Neurol.*, 178 (1978) 49–72.
51 Garcia-Sanchez, J. L., Buño, W. Jr., Fuentes, J. and Garcia-Austt, E., Nonrhythmical hippocampal units, theta rhythm, and afferent stimulation, *Brain Res. Bull.*, 3 (1978) 213–219.
52 Gayoso, M. F., Dias-Flores, L., Garrido, M., Sanchez, G. and Velasco, E., Hippocampal formation. IV. Interneurons, *Morf. Normal Path.*, 3 (1979) 247–277.
53 Gerbrandt, L. K., Lawrence, F. C., Fowler, F. R. and Weyand, T. G., Multiple origins of the hippocampal theta rhythm, *Proc. Soc. Neurosci. Abstr.*, 4 (1974) 230.
54 Gogolak, G., Stumpf, C. H., Petsche, H. and Sterc, F., The firing patterns of septal neurons and the form of hippocampal theta wave, *Brain Research*, 7 (1968) 201–207.
55 Grantyn, A. and Grantyn, R., Postsynaptic responses of hippocampal neurons to subcortical stimulation: differentiation of ascending pathways, *Acta physiol. Acad. Sci. hung.*, 43 (1973) 329–345.
56 Grastyán, E., Lissák, K., Madarász, I. and Donhoffer, H., Hippocampal electrical activity during the development of conditioned reflexes, *Electroenceph. clin. Neurophysiol.*, 11 (1959) 409–430.
57 Green, J. D. and Arduini, A., Hippocampal electrical activity in arousal, *J. Neurophysiol.*, 17 (1954) 533–557.
58 Green, J. D. and Machne, X., Unit activity of rabbit hippocampus, *Amer. J. Physiol.*, 181 (1955) 219–224.
59 Green, J., Maxwell, D. S., Schindler, W. J. and Stumpf, C., Rabbit EEG 'theta' rhythm: its anatomical source and relation to activity in single neurons, *J. Neurophysiol.*, 23 (1960) 403–420.
60 Hjorth-Simonsen, A., Distribution of commissural afferents to the hippocampus of the rabbit, *J. comp. Neurol.*, 176 (1977) 495–514.

61 Holsheimer, J., Boer, J., Lopes da Silva, F. H. and Van Rotterdam, A., The double dipole model of theta rhythm generation: simulation of laminar field potential profiles in dorsal hippocampus of the rat, *Brain Research,* 235 (1982) 31–50.

62 Holst, E. von, and Saint Paul, U. von, Das Reaffenzprinzip, *Naturwissenschaften,* 37 (1950) 464–476.

63 Isaacson, R. L., *The Limbic System (2nd edn.),* Plenum Press, New York, 1982.

64 Isaacson, R. L. and Pribram, K. H. (Eds.), *The Hippocampus, Vols. 1 and 2,* Plenum, New York, 1975.

65 Ito, M. and Olds, J., Unit activity during self-stimulation behavior, *J. Neurophysiol.,* 34 (1971) 263–273.

66 Kandel, E. R. and Spencer, W. A., Electrophysiology of hippocampal neurons. II. Afterpotentials and repetitive firing, *J. Neurophysiol.,* 24 (1961) 243–259.

67 Klemm, W. R., Hippocampal EEG and information processing. A special role for theta rhythm, *Prog. Neurobiol.,* 7 (1976) 197–214.

68 Knowles, W. D. and Schwartzkroin, P. A., Local circuit synaptic interactions in hippocampal brain slices, *J. Neurosci.,* 1 (1981) 318–322.

69 Knowles, W. D. and Schwartzkroin, P. A., Axonal ramifications of hippocampal CA1 pyramidal cells, *J. Neurosci.,* 1 (1981) 1236–1241.

70 Kramis, R., Vanderwolf, C. H. and Bland, B. H., Two types of hippocampal rhythmical slow activity in both the rabbit and the rat: relations to behavior and effects of atropine, diethyl ether, urethane and pentobarbital, *Exp. Neurol.,* 49 (1975) 58–85.

71 Kuhar, M. J. and Yamamura, H. I., Light autoradiographic localization of cholinergic muscarinic receptors in rat brain by specific binding of a potent antagonist, *Nature (Lond.),* 253 (1965) 560–561.

72 Laatsch, R. H. and Cowan, W. M., Electron microscopic studies of the dentate gyrus of the rat. II. Degeneration of commissural afferents, *J. comp. Neurol.,* 120 (1967) 241–261.

73 Laurberg, S., Commissural and intrinsic connections of the rat hippocampus, *J. comp. Neurol.,* 184 (1979) 685–708.

74 Laurberg, S. and Sørensen, K. E., Associational and commissural collaterals of neurons in the hippocampal formation (hilus fasciae dentata and subfield CA3), *Brain Research,* 212 (1981) 287–300.

75 Lebovitz, R. M., Dichter, M. and Spencer, W. A., Recurrent excitation in the CA3 region of cat hippocampus, *Int. J. Neurosci.,* 2 (1971) 99–108.

76 Leung, L. S., Potentials evoked by alvear tract in hippocampal CA1 region of rats II. Spatial field analysis, *J. Neurophysiol.,* 42 (1979) 1571–1589.

77 Leung, L. S., Nonlinear feedback model of neuronal populations in the hippocampal CA1 region, *J. Neurophysiol.,* 47 (1982) 845–868.

78 Leung, L. S., Lopes da Silva, F. H. and Wadman, W. J., Spectral characteristics of the hippocampal EEG in the freely moving rat, *Electroenceph. clin. Neurophysiol.,* 54 (1982) 203–219.

79 Lidsley, T. I., Levine, M. S. and MacGregor, S. Jr., Hippocampal units during orienting and arousal in rabbits, *Exp. Neurol.,* 44 (1974) 171–186.

80 Lømo, T., Patterns of activation in a monosynaptic cortical pathway: the perforant path input to the dentate area of the hippocampal formation, *Exp. Brain Res.,* 12 (1971) 18–45.

81 Lopes da Silva, F. H. and Arnolds, D. E. A. T., The physiology of the hippocampus and related structures, *Ann. Rev. Physiol.,* 40 (1978) 163–191.

82 Lopes da Silva, F. H., Van Rotterdam, A., Barts, P., Van Heusden, E. and Burr, W., Models of neuronal populations: the basic mechanisms of rhythmicity. *Prog. Brain Res.,* 45 (1976) 281–308.

83 Lorente de Nó, R., Studies on the structure of the cerebral cortex. II. Continuation of the study of the Ammonic system, *J. Psychol. Neurol.,* 46 (1934) 113–177.

84 Lynch, G., Rose, G. and Gall, C., Anatomical and functional aspects of the septo-hippocampal projections. In: *CIBA Symposium 58, Functions of the septo-hippocampal system,* Elsevier, Amsterdam, 1978, pp. 5–20.

85 Macadar, O., Roig, J. A., Monti, J. M. and Budelli, R., The functional relationship between septal and hippocampal unit activity and hippocampal theta rhythm, *Physiol. Behav.,* 5 (1970) 1443–1449.

86 MacLean, P. D., An ongoing analysis of hippocampal inputs and outputs: microelectrode and neuroanatomical findings in squirrel monkeys. In R. L. Isaacson and K. H. Pribram (Eds.), *The Hippocampus Vol. 1,* Plenum Press, New York, 1975, pp. 177–211.

87 MacVicar, B. A. and Dudek, F. E., Electronic coupling between pyramidal cells: a direct demonstration in rat hippocampal slices, *Science,* 213 (1981) 782–785.

88 Mathisen, J. S. and Blackstad, T. W., Cholinesterase in the hippocampal region. Distribution and relation to architectonics and afferent systems, *Acta anat.,* 56 (1964) 216–253.

89 Mays, L. E. and Best, P. J., Hippocampal unit activity to tonal stimuli during arousal from sleep and in awake rats, *Exp. Neurol.,* 47 (1975) 268–279.

90 McNaughton, B. L. and Barnes, C. A., Physiological identification and analysis of dentate granule cell responses to stimulation of the medial and lateral perforant pathways in the rat, *J. comp. Neurol.,* 175 (1977) 439–454.

91 Meibach, R. C. and Siegel, A., Efferent connections of the septal area in the rat: an analysis utilizing retrograde and anterograde transport methods, *Brain Research,* 119 (1977) 1–20.

92 Mellgren, S. I. and Srebro, B., Changes in acetylcholinesterase and distribution of degenerating fibers in the rat hippocampal region after septal lesions in the rat, *Brain Research,* 52 (1973) 19–36.

93 Miller, V. M. and Best, P. J., Spatial correlates of hippocampal unit activity are altered by lesions of the fornix and entorhinal cortex, *Brain Research,* 194 (1980) 311–323.

94 Mink, W. D., Best, P. J. and Olds, J., Neurons in paradoxical sleep and motivated behavior, *Science,* 158 (1967) 1335–1337.

95 Mitchell, S. and Ranck, J. B. Jr., Generation of theta rhythm in medial entorhinal cortex of freely moving rats, *Brain Research,* 189 (1980) 49–66.

96 Moiseeva, N. I., Alexanian, Z. A. and Matveev, T. K., Spontaneous activity of neuronal assemblies in subcortical structures during sleeping and dreaming in man, *Sechenov physiol. J. U.S.S.R.,* 52 (1971) 159–166.

97 Mosko, S., Lynch, G. and Cotman, C. W., The distribution of septal projections to the hippocampus of the rat, *J. comp. Neurol.,* 152 (1973) 163–174.

98 Nunzi, M. G., Gorio, A., Smith, D. A. and Somogyi, P., A specific interneuron forming synapses exclusively with the axon initial segment of pyramidal cells in monkey hip-

pocampus, *Soc. Neurosci. Abstr.*, 8 (1982) 216.
99 O'Keefe, J., Place units in the hippocampus of the freely moving rat, *Exp. Neurol.*, 51 (1976) 78–109.
100 O'Keefe, J. and Nadel, L., *The hippocampus as a cognitive map*, Clarendon Press, Oxford, 1978.
101 Olmstead, C. E., Best, P. J. and Mays, L. E., Neural activity in the dorsal hippocampus during paradoxical sleep, slow wave sleep and waking, *Brain Research*, 60 (1973) 381–391.
102 Petsche, H., Stumpf, C. and Gogolak, G., The significance of the rabbit's septum as a relay station between the midbrain and the hippocampus. The control of hippocampus arousal activity by septum cells, *Electroenceph. clin. Neurophysiol.*, 14 (1962) 202–211.
103 Prince, D. A., Neurophysiology of epilepsy, *Ann. Rev. Neurosci.*, 1 (1978) 395–415.
104 Ramón y Cajal, S., *Histologie du Système Nerveux de l'Homme et des Vertébrés, Vol. 2*, Maloine, Paris, 1911.
105 Ranck, J. B. Jr., Studies on single neurons in dorsal hippocampal formation and septum in unrestrained rats, I. Behavioral correlates and firing repertoires, *Exp. Neurol.*, 42 (1973) 461–531.
106 Rappelsberger, P., Pockberger, H. and Petsche, H., The contribution of the cortical layers to the generation of the EEG: field potential and current source density analyses in the rabbit's visual cortex, *Electroencephal. clin. Neurophysiol.*, 53 (1982) 254–269.
107 Ribak, C. E. and Anderson, L., Ultrastructure of the pyramidal basket cells in the dentate gyrus of the rat, *J. comp. Neurol.*, 192 (1980) 903–916.
108 Ribak, C. E. and Seress, L., Commissural axons synapse with indentified basket cells in the rat dentate gyrus: a combined degeneration–Golgi–electron microscopic study, *Soc. Neurosci. Abstr.*, 8 (1982) 836.
109 Ribak, C. E. and Seress, L., Five types of basket cells in the hippocampal dentate gyrus. A combined Golgi and electron microscopic study, *J. Neurocytol.*, in press.
110 Ribak, C. E., Vaugh, J. E. and Saito, K., Immunocytochemical localization of glutamic acid decarboxylase in neuronal somata following colchicine inhibition of axonal transport, *Brain Research*, 140 (1978) 315–332.
111 Rose, G. M., *Physiological Analysis of the Hippocampus During Behavior*, Doctoral Dissertation, University of California, Irvine, 1980 (unpublished).
112 Rose, G. and Schubert, P., Release and transfer of [^{3}H]adenosine derivatives in the cholinergic septal system, *Brain Research*, 12 (1977) 353–357.
113 Schaffer, K., Beitrag zur Histologie der Ammonshorn Formation, *Arch. Mikrosk. Anat.*, 39 (1982) 611–632.
114 Schwartzkroin, P. A. and Mathers, L. H., Physiological and morphological identification of a nonpyramidal hippocampal cell type, *Brain Research*, 157 (1978) 1–10.
115 Segal, M. and Landis, S., Afferents to the hippocampus studied with the method of retrograde transport of horseradish peroxidase, *Exp. Neurol.*, 78 (1974) 1–15.
116 Seress, K., Pyramid-like basket cells in the granular of the dentate gyrus in the rat, *J. Anat.*, 127 (1978) 163–168.
117 Seress, L. and Pokorny, F., The structure of the granular layer of the rat dentate gyrus. A light microscopic and Golgi study, *J. Anat.*, 133 (1981) 181–195.
118 Seress, L. and Ribak, C. E., GABAergic cells in the dentate gyrus appear to be local circuit and projection neurons, *Exp. Brain Res.*, 50 (1983) 173–182.
119 Sinclair, B. R., Seto, M. G. and Bland, B. H., Theta cells in the CA1 and dentate layers of the hippocampal formation: relations to slow wave activity and motor behavior in the freely moving rabbit, *J. Neurophysiol.*, 48 (1982) 1214–1225.
120 Spencer, W. A. and Kandel, E. R., Hippocampal neuron responses to selective activation of recurrent collaterals of hippocampal axons, *Exp. Neurol.*, 4 (1961) 149–161.
121 Steward, O., Topographical organization of the projections from the entorhinal area to the hippocampal formation of the rat, *J. comp. Neurol.*, 167 (1976) 285–314.
122 Steward, O., Cells of origin of entorhinal cortical afferents to the hippocampus and fascia dentata of the rat, *J. comp. Neurol.*, 169 (1976) 347–370.
123 Storm-Mathisen, J., Quantitative histochemistry of acetylcholinesterase in rat hippocampal region correlated to histochemical staining, *J. Neurochem.*, 17 (1970) 739–750.
124 Struble, R. G., Desmond, N. L. and Levy, W. B., Anatomical evidence for interlamellar inhibition in the fascia dentata, *Brain Research*, 152 (1978) 580–585.
125 Stumpf, C., Drug action on the electrical activity of the hippocampus, *Int. Rev. Neurobiol.*, 8 (1965) 77–138.
126 Suzuki, S. S. and Smith, G. K., Spontaneous EEG spikes in the hippocampus of normal behaving rat, *Soc. Neurosci. Abstr.*, 8 (1982) 1017.
127 Swanson, L. W. and Cowan, W. M., An autoradiographic study of the organization of the efferent connections of the hippocampal formation in the rat, *J. comp. Neurol.*, 172 (1977) 49–84.
128 Swanson, K. W. and Cowan, W. M., The connections of the septal region in the rat, *J. comp. Neurol.*, 186 (1979) 621–656.
129 Swanson, L. W., Sawchenko, P. E. and Cowan, W. M., Evidence for collateral projections by neurons in Ammon's horn, the dentate gyrus, and the subiculum: a multiple retrograde labeling study in the rat, *J. Neurosci.*, 1 (1981) 548–559.
130 Swanson, L. W., Wyss, F. M. and Cowan, W. M., An autoradiographic study of the organization of intrahippocampal association pathways in the rat, *J. comp. Neurol.*, 181 (1978) 681–716.
131 Traub, R. D. and Wong, R. K. S., Cellular mechanism of neuronal synchronization in epilepsy, *Science*, 216 (1982) 745–747.
132 Turner, D. A. and Schwartzkroin, P. A., Steady-state electronic analysis of intracellularly stained hippocampal neurons, *J. Neurophysiol.*, 44 (1980) 184–199.
133 Vanderwolf, C. H., Hippocampal electrical activity and voluntary movement in the rat, *Electroenceph. clin. Neurophysiol.*, 26 (1969) 407–418.
134 Vanderwolf, C. H., Kramis, R. and Robinson, T. E., Hippocampal electrical activity during waking behaviour and sleep: analyses using centrally acting drugs, In *Functions of the Septo-Hippocampal System*, CIBA Foundation Symposium, 58 (1978) 199–226.
135 Vanderwolf, C. H. and Leung, L. S., Hippocampal rhythmical slow activity. A brief history and the effects of entorhinal lesions and phencyclidine. In W. Seifert (Ed.), *Molecular, Cellular and Behavioral Neurobiology of the Hippocampus*, Academic Press, New York, 1983.
136 Vanderwolf, C. H. and Leung, L. S., Effects of entorhinal, cingulate and neocortical lesions on atropine resistant hippocampal RSA, *Neurosci. Lett.*, Suppl. 10 (1982) S501.

137 Van Hoesen, G. W., Pandya, D. N. and Butters, N., Cortical afferents to the entorhinal cortex of the rhesus monkey, *Science*, 175 (1972) 1471–1473.
138 Vijayan, V. K., Distribution of cholinergic neurotransmitter enzymes in the hippocampus and the dentate gyrus of the adult and developing mouse, *Neuroscience*, 4 (1979) 121–137.
139 West, J. R., Nornes, H. O., Barnes, C. L. and Bronfenbrenner, B., The cells of origin of the commissural afferents to the area dentata in the mouse, *Brain Research*, 160 (1979) 203–215.
140 Whishaw, I. Q. and Sutherland, R. J., Sparing of rhythmic slow wave activity (RSA or *theta*) in two hippocampal generators after kainic acid CA3 and CA4 lesions, *Exp. Neurol.*, 75 (1982) 711–728.
141 Winson, J., Patterns of hippocampal theta in the freely moving rat, *Electroenceph. clin. Neurophysiol.*, 36 (1974) 291–301.
142 Winson, J. and Abzug, C., Neuronal transmission through hippocampal pathways dependent on behavior, *J. Neurophysiol.*, 41 (1978) 716–732.
143 Wolfson, S., Fox, S. E. and Ranck, J. B. Jr., Theta cells in dorsal CA1, CA3, and dentate fire maximally on the positive phase of dentate theta rhythm in walking rats, *Soc. Neurosci. Abstr.*, 5 (1979) 284.
144 Wolfson, S., Fox, S. E. and Ranck, J. B., Jr., Hippocampal theta rhythm: phase-relations of neuron firing and conductance in urethanized rats, *Soc. Neurosci. Abstr.*, 7 (1981) 451.
145 Wong, R. K. S. and Prince, D. A., Afterpotential generation in hippocampal pyramidal cells, *J. Neurophysiol.*, 45 (1981) 86–97.